

Triple Recognition of B-DNA by a Neomycin–Hoechst 33258–Pyrene Conjugate[†]

Bert Willis and Dev P. Arya*

Laboratories of Medicinal Chemistry, Clemson University, Clemson, South Carolina 29634

Received September 25, 2009; Revised Manuscript Received November 21, 2009

ABSTRACT: Recent developments have indicated that aminoglycoside binding is not limited to RNA, but to nucleic acids that, like RNA, adopt conformations similar to its A-form. We further sought to expand the utility of aminoglycoside binding to B-DNA structures by conjugating neomycin, an aminoglycoside antibiotic, with the B-DNA minor groove binding ligand Hoechst 33258. Envisioning a dual groove binding mode, we have extended the potential recognition process to include a third, intercalative moiety. Similar conjugates, which vary in the number of binding moieties but maintain identical linkages to allow direct comparisons to be made, have also been prepared. We report herein novel neomycin- and Hoechst 33258-based conjugates developed in our laboratories for exploring the recognition potential with B-DNA. Spectroscopic studies such as UV melting, differential scanning calorimetry, isothermal fluorescence titrations, and circular dichroism together illustrate the triple recognition of the novel conjugate containing neomycin, Hoechst 33258, and pyrene. This study represents the first example of DNA molecular recognition capable of minor versus major groove recognition in conjunction with intercalation.

Targeting genes with small molecules has gradually become a reality in medicine, because of a deeper understanding of the structure and sequence of DNA. For example, the action of drugs such as anthracyclines and acridines (both DNA intercalators) involves the binding and stabilization of ternary complexes of DNA with DNA topoisomerases, a phenomenon unknown until recently (1–4). The understanding of recognition in structure-specific and DNA sequence-specific binding modes is crucial to defining the principles for consistent development of gene regulatory drugs.

The minor groove is perhaps the most studied of the potential sites of recognition of DNA by small molecules over the past decade (5). Exploiting solid phase synthesis techniques for preparation of polyamides based on distamycin and netropsin, Dervan (6, 7) has set forth rules for base pairing recognition centralized on tandem interactions between imidazole and/or pyrrole pairs formed via polyamide dimers or hairpin structures. A promising feature of such polyamides, because of their high affinities for B-DNA, is their ability to compete with specific protein–DNA binding (8–13). The inhibition is not limited to minor groove binding transcription factors; polyamide binding may also succeed at “locking” DNA into its B-form such that major groove binding proteins may fail in their attempt to distort the B-DNA conformation upon binding (8).

Gene regulation by small molecules is driven by the development of ligands that bind unique stretches of DNA. Extending beyond the conventional polyamide hairpins and bis(benzimidazoles) for recognition of up to 6 bp, current research has uncovered a few remarkable conjugates that have been shown to recognize longer stretches of DNA. For example, head-to-head hairpin polyamide dimers have been shown to recognize DNA from 10 to 12 bp in length (14). Utilizing the ability of

pyrrole/imidazole or hydroxypyrrrole/pyrrole (15) pairs to discriminate base pair recognition, Dervan has shown that 5'-TGGCATAACCA-3', 5'-TGGCATTACCA-3', and 5'-TGGCATATACCA-3' can bind hairpin dimers at subnanomolar concentrations (14).

Another well-studied minor groove binding structural motif is bis(benzimidazole), originating from the early discoveries of compounds such as Hoechst 33258 binding to DNA (16, 17). These benzimidazoles are known for their potential to poison DNA topoisomerases or to stabilize complexes of DNA topoisomerases that ultimately result in strand cleavage (18). Numerous reports on benzimidazoles exist, ranging from tris(benzimidazoles) (19, 20) to furamidine-benzimidazole (21–23) structures, as well as conjugates with distamycin (among other polyamides), polyamines (24) (including our work with neomycin-conjugated Hoechst 33258) (25, 26), and intercalators. Minor groove binder–polyamine conjugates have prospects for dual binding of DNA, by binding both the minor groove and the major groove (polyamine) in tandem (24, 27–30). We recently showed that neomycin can be driven to bind the B-DNA major groove when conjugated with the minor groove binding Hoechst 33258 (25, 26).

A number of natural products have been shown to possess structures characteristic of both groove binding and intercalation. Selected examples (Figure 1) include rebeccamycin (indolecarbazole family), nogalamycin (anthracycline family), altromycin (pluramycin family), and mithramycin (aureolic acid family). Some include an additional electrophilic moiety capable of alkylating DNA. Furthermore, the majority have been shown to display multiple DNA binding modes. For example, nogalamycin has recently been reported to thread DNA, exhibiting intercalation by the central chromophore, with saccharide regions extending from both ends to bind both major and minor grooves.

In addition to their well-known potential as RNA-targeted drugs, we have utilized aminoglycosides for probing nucleic acid recognition in a variety of pathways (31–42). By utilizing

[†]We are grateful to the National Science Foundation (CHE 0134792) for financial support.

*To whom correspondence should be addressed. E-mail: dparya@clemson.edu. Phone: (864) 656-1106. Fax: (864) 656-6617.

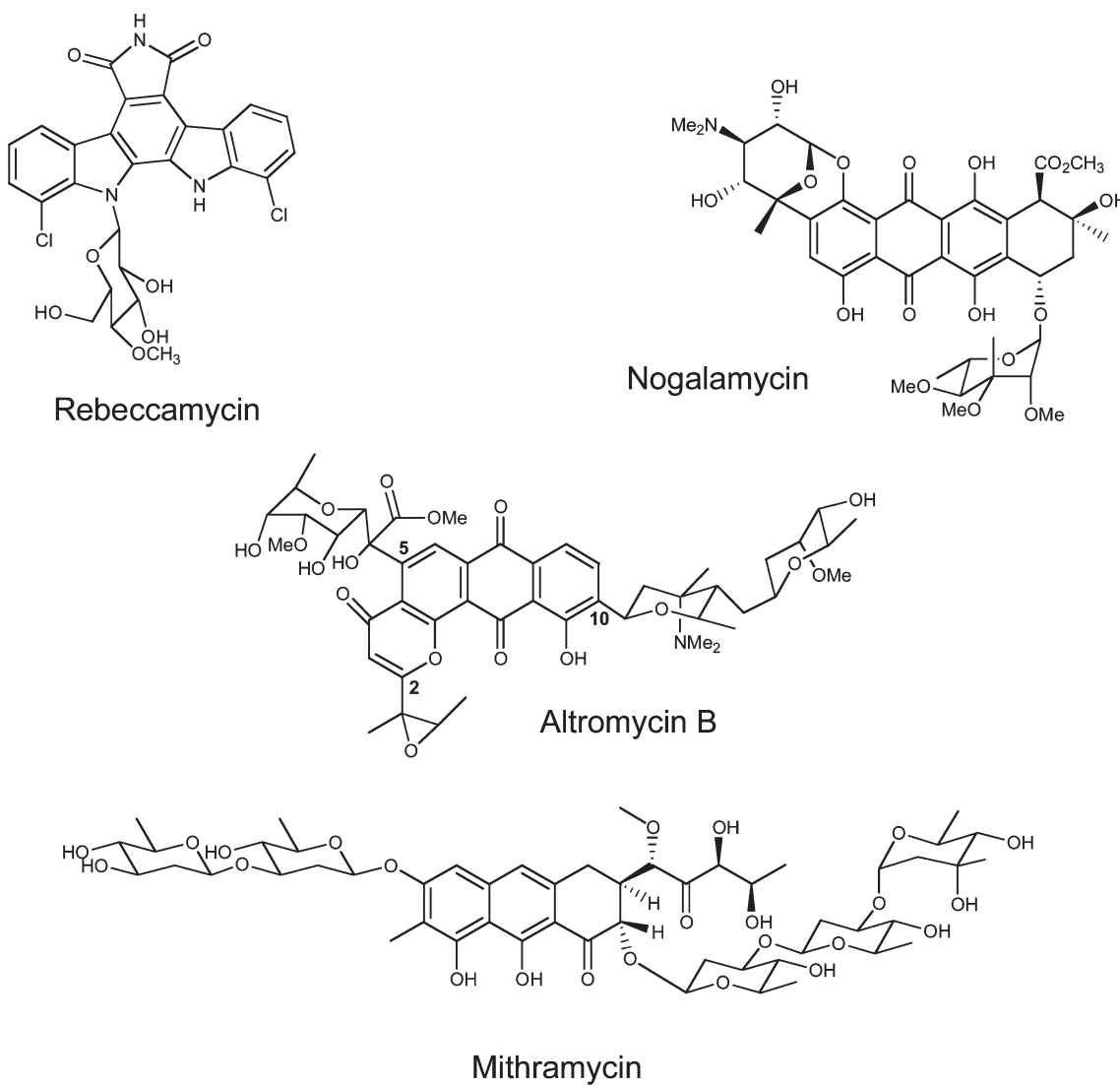


FIGURE 1: Structures of naturally occurring intercalator–groove binder hybrids that bind DNA.

synthetic neomycin intermediates for their covalent attachment with intercalators [pyrene (43, 44), BQQ (44), and methidium (45, 46)] and groove binders [Hoechst 33258 (25, 26) and DNA (47, 48)], we have shown an increased binding affinity for both A-form (or A-like) and B-form nucleic acids (25, 26). We extend the recognition potential by combining major groove binding of neomycin with both intercalating and minor groove binding moieties in one molecule (49). Outlined in the forthcoming article are advancements toward multi-recognition of DNA by the successful design, synthesis, and binding studies of a novel neomycin–Hoechst 33258–pyrene conjugate, termed “NHP”. For the sake of comparison, control compounds lacking one of the binding moieties were also prepared. A combination of spectroscopic, calorimetric, and viscometric techniques were utilized in probing the binding properties of these novel ligands. Results show that NHP is the first ligand designed to simultaneously recognize DNA via all three recognition motifs: major groove, minor groove, and intercalation.

EXPERIMENTAL PROCEDURES

Materials. (i) *Nucleic Acids.* Oligonucleotides were purchased from Integrated DNA Technologies and used without further purification. Polymeric DNA [poly(dA)·poly(dT), lot

4117860021] was purchased from Amersham Pharmacia (Piscataway, NJ). All concentrations were determined spectrophotometrically using extinction coefficients provided by the supplier.

(ii) *Chemicals.* Neomycin B (sulfate salt) was purchased from ICN pharmaceuticals and used without further purification (both synthesis and binding experiments); DIAD (diisopropylazodicarboxylate) and 1,1'-thiocarbonyldi-2(1*H*)-pyridone were purchased from Aldrich Chemical Co. All other reagents and solvents were purchased from Acros Organics and used without further purification. Reaction solvents were distilled accordingly; methylene chloride and pyridine were distilled over calcium hydride, and diethyl ether and 1,4-dioxane were distilled over sodium metal. Conjugate NH was synthesized as reported previously (26). Quantitation of Hoechst 33258 ($\epsilon_{338} = 42000 \text{ M}^{-1} \text{ cm}^{-1}$), NH ($\epsilon_{342} = 39241 \text{ M}^{-1} \text{ cm}^{-1}$), NH ($\epsilon_{342} = 21085 \text{ M}^{-1} \text{ cm}^{-1}$), and NHP ($\epsilon_{345} = 53674 \text{ M}^{-1} \text{ cm}^{-1}$) in aqueous solutions was conducted using UV absorbance. To ensure stability and minimum adsorption of Hoechst compounds to container walls, all solutions were stored in nontransparent, polystyrene tubes.

Methods. (i) *UV Melting.* Samples of DNA (1 μM in duplex for oligomers, 15 μM for polymers) were mixed with ligand in buffer before being heated at 95 °C for 5 min and slowly annealed to 20 °C. UV analysis was then conducted at 260 nm

from 20 to 95 °C at a heating rate of 0.2 °C/min. T_m values were determined by first-derivative analysis (where clearly discerned) using instrument software or via the midpoint of the transition where broad transitions were observed.

(ii) *Fluorescence Titrations.* Equilibrium binding experiments were conducted using a Photon Technology International (Lawrenceville, NJ) instrument at ambient temperature (22 °C). A solution of ligand (serially diluted to working concentrations) was excited at its respective λ_{max} (slits of 3 nm), and resulting emission curves (from 390 to 600 nm) were recorded after serial additions of a concentrated DNA solution [poly(dA)·poly(dT)] was 200 μM base⁻¹. After each addition, the solution was mixed by pipetting up and down with a Pasteur pipet treated with silanizing agent (SigmaCote) to avoid adsorption of ligand to the glass. Sample equilibrium was monitored by continually exciting and scanning the sample at different times and was usually reached within 2 min. All data were normalized to account for the (small) dilution of sample upon addition of substrate. For the self-complementary 12mer experiments, individual samples of varying ligand:DNA ratios were prepared, all with a constant ligand concentration of 100 nM. A silanized (SigmaCote) or polystyrene cuvette was used in all experiments. Corresponding fluorescence data were fit using Kaleidagraph (see the Supporting Information for further details of the curve fitting).

(iii) *CD Spectropolarimetry Titrations.* Circular dichroism (CD) experiments were conducted at 20 °C using a Jasco J-810 spectropolarimeter. A concentrated solution of ligand (200 μM) was added to a 30 μM solution of poly(dA)·poly(dT) and the mixture stirred constantly before being scanned from 450 to 210 nm. As with fluorescence experiments, equilibrium was determined by periodically scanning the sample over a period of time (up to 10 min) for the first few additions of ligand and was reached within 3 min. An average of three scans were gathered for each titration point. All data were normalized to account for the (small) dilution of sample upon addition of ligand.

(iv) *Viscometry.* Viscosity measurements were conducted using a Cannon-Ubbelohde 75 capillary viscometer submerged in a water bath at 27 ± 0.05 °C. Flow times of buffer only followed by DNA (1030 μL of a 100 μM solution in base pairs) were recorded in triplicate before titrations of concentrated ligand solutions (500 μM) with mixing by bubbling of air (using a pipet bulb) through the solution. Flow times after each titration were recorded in triplicate. In all cases, standard deviations were less than 0.1 s. All solutions were in 10 mM sodium cacodylate buffer containing 150 mM KCl and 1 mM MgCl₂ (pH 7.2). Flow times for buffer alone were in the range of 106 s, whereas the flow time for DNA alone was approximately 112 s. Flow times for titrations of ligand into DNA ranged from 110 to 108 s. The viscosity for each titration was determined using a protocol similar to that reported previously (50). For further explanation of the analysis, please see the Supporting Information.

(v) *Differential Scanning Calorimetry.* DSC experiments were conducted on a MicroCal VP-DSC instrument. Samples of DNA (512 μL of a 100 μM solution in base pairs) in the absence and presence of ligand (8 μM) were heated from 20 to 110 °C at a scan rate of 30 °C/h. After buffer subtraction (usually negligible), baseline adjustments, T_m assignments, and peak integrations were conducted using Origin version 5.0. For further explanation of the analysis, see the Supporting Information.

(vi) *Computer Modeling.* The DNA duplex d(CGCAATTGCG)₂ was extracted from Protein Data Bank (PDB) entry 296d (51). Conformational optimization of neomycin,

docked closest to its 5' position for the Hoechst linker, was conducted prior to attachment to Hoechst using a Monte Carlo routine in MacroModel, using the AMBER* force field and water as the solvent. A similar protocol was used for the Hoechst 33258 and pyrene moieties. Five of the six amines in neomycin were protonated, in agreement with NMR studies of neomycin (52, 53), as well as the terminal amine in the piperazine ring of the Hoechst moiety. Three MC runs (for all single bond torsional angles and 1000 steps each) starting from different initial conformations were conducted, yielding the same global minimum conformation. All the flexible bonds were selected. The ligands were built and optimized in Macromodel, and the RESP charges were derived using ab initio calculations with a 6-31 G* basis set in Jaguar. The minimized complexes were then reminimized with the distance constraints removed to a root-mean-square gradient of 0.08 kcal mol⁻¹ Å⁻² to allow unfavorable contacts to be removed. In the next step, all the restrictions were removed except the movement of ring atoms of the terminal bases and energy minimization reached a convergence threshold of 0.05 kJ/mol in all cases. After structural minimization, the data file was imported into WebLabViewer and the surface potential of the complex was rendered using WebLabViewer.

Synthesis. For synthesis of all intermediates, see the Supporting Information.

(i) *HPA (3).* Compound **10** was converted to the corresponding imidate ethyl ester by vigorously bubbling anhydrous HCl into a solution of **10** in dry EtOH for 30 min before being stored at 4 °C overnight. After acid removal (bubbling nitrogen through the solution into a saturated bicarbonate solution) and EtOH evaporation, the imidate was rinsed well with dry ether before being dried in *vacuo* and used immediately without characterization.

To the corresponding imidate of **10** were added diamine **11** and a 3:1 dry EtOH/glacial acetic acid solution (2 mL) before the mixture was refluxed for 8 h under argon. The acetic acid was removed, and the crude mixture was loaded onto a column of silica before purification using a gradient of MeOH (0 to 15%) in CH₂Cl₂ containing a trace of NEt₃. The product *N*-trifluoroacetamide of **3** is represented by an intense yellow-green fluorescence under long UV. R_f = 0.6 (85:15:0.1 CH₂Cl₂/MeOH/NH₄OH). Unknown benzimidazole byproducts, fluorescent purple under long UV, were difficult to separate; therefore, the crude product was deprotected as indicated below, with full characterization. MALDI-MS confirmed the product: [M]⁺ 1053.18, found 1053.00.

Deprotection of the corresponding trifluoroacetamide (14 mg, 13.3 μmol) was eliminated when the solution was stirred with a 2:1 mixture of MeOH and water (1.5 mL) containing K₂CO₃ (25 mg, 0.18 mmol) for 24 h before solvent removal, dissolution in MeOH and filtration, and further coevaporation of MeOH with toluene (2 × 3 mL) and purified over a short column of silica with a gradient from 20 to 50% MeOH in CH₂Cl₂ until less polar impurities were flushed off (which fluoresced purple under long UV) before elution of a 1:1 CH₂Cl₂/MeOH mixture containing 2% NEt₃. Product fluoresces yellow-green under long UV. After evaporation of solvent and a rinse with ether, 12 mg (94%) of the pure amine **3** was obtained: ¹H NMR (500 MHz, CDCl₃) δ 8.44 (d, 1H, *J* = 8.7 Hz), 8.25–7.90 (m, 12H), 7.48–7.38 (m, 1H), 7.30–6.93 (m, 5H), 4.13 (m, 2H), 3.80–3.10 (m, 22H, peaks masked by solvent signal), 2.93–2.89 (m, 4H), 2.05–1.95 (m, 2H); MS (MALDI-TOF) *m/z* for C₅₇H₆₄N₈O₆ [M]⁺ 957.17, found 957.77.

(ii) *NHP 4.* To the Boc-protected conjugate **13** (5 mg, 2.2 μmol) were added dry CH₂Cl₂ (1 mL) and trifluoroacetic

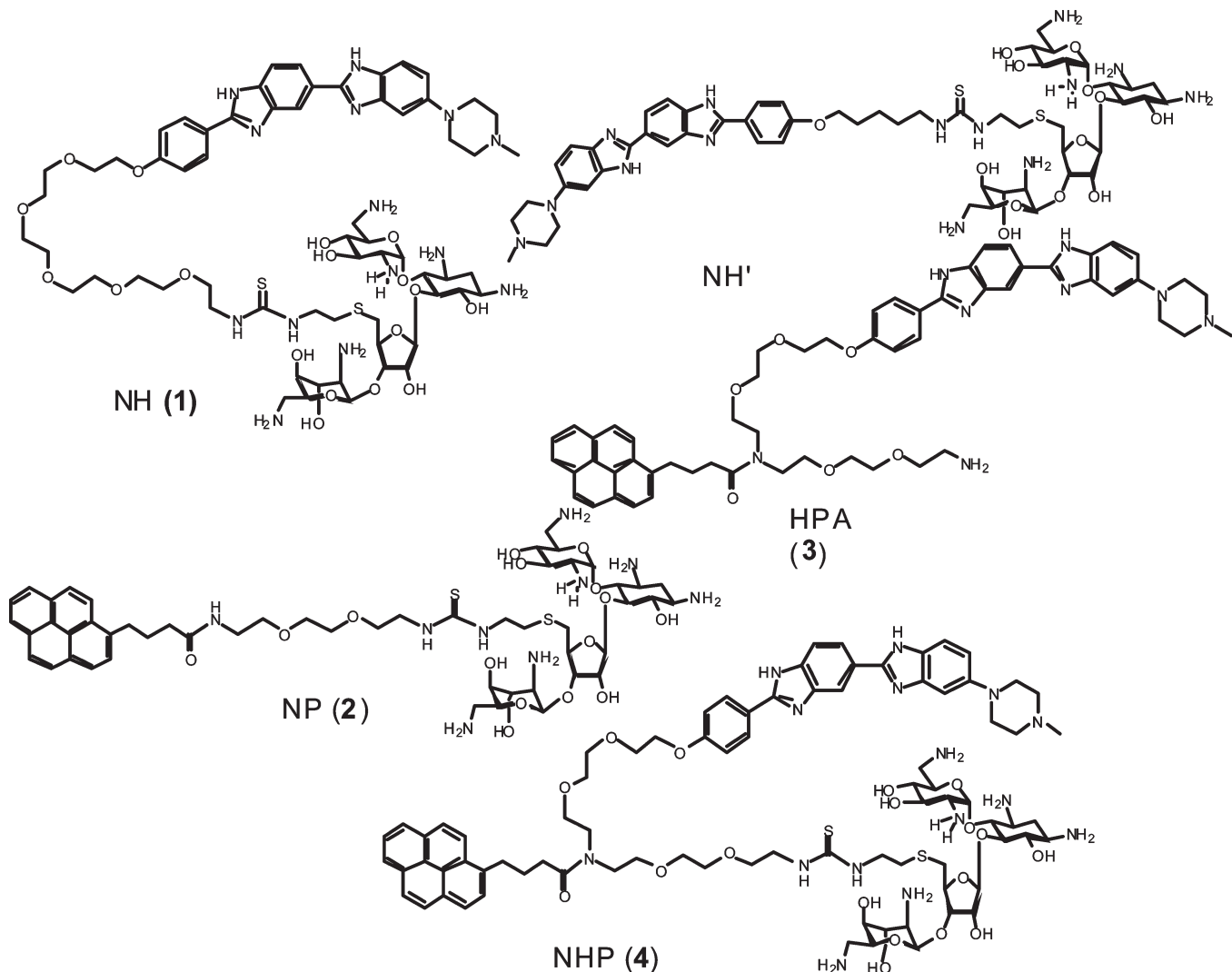


FIGURE 2: Structures of novel conjugates used in this study.

acid (1 mL) and 5 μ L of ethanedithiol as a scavenger before the mixture was stirred at room temperature for 3 h. Evaporation of liquids and addition of ether gave a light brown solid which, after subsequent rinses with ether and being dried under vacuum, was dissolved in deionized water and lyophilized to afford 6 mg of product (quant.). The product was judged to be sufficiently pure by analytical HPLC (Supelcosil LC18S column; eluent, 0.1% aqueous TFA with a gradient from 0 to 100% of a 95:5 acetonitrile/water mixture over a period of 20 min; flow rate, 1.2 mL/min; ambient temperature; retention time of product, 8.9 min): ^1H NMR (500 MHz, D₂O with CF₃CO₂D) δ 8.66 (br s, 1H), 8.51 (br s, 1H), 7.96 (br s, 1H), 7.52–6.30 (d, 14H), 5.96–5.80 (m, 3H), 5.30 (s, 1H), 4.10–2.97 (m, 52H), 2.64–2.17 (m, 5H), 1.98–1.92 (m, 2H), 1.85–1.70 (m, 2H); MS (MALDI-TOF) m/z for C₈₃H₁₁₃N₁₅NaO₁₈S₂ [M + Na]⁺ 1696.0, found 1696.6; UV (water) λ_{max} = 345 nm (ϵ = 53674 M⁻¹ cm⁻¹).

(iii) Compound 2 (NP). A solution of **15** (5 mg, 2.88 μ mol) was stirred in a 1:1 mixture of dry CH₂Cl₂ and TFA containing a trace of ethanedithiol at room temperature, under N₂ for 3 h. The liquids were evaporated, and the solid was taken up in deionized water before lyophilization to afford 5 mg of product (96%). The product was judged to be sufficiently pure by analytical HPLC (Supelcosil LC18S column; eluent, 0.1% aqueous TFA with a gradient from 5 to 100% acetonitrile over a period of 20 min; flow rate, 1.5 mL/min; ambient temperature; retention time of product,

14.6 min): ^1H NMR (500 MHz, D₂O) δ 8.38 (d, 1H, J = 9.2 Hz), 8.28 (t, 2H, J = 6.9 Hz), 8.23 (d, 2H, J = 8.3 Hz), 8.13 (s, 2H), 8.09 (t, 1H, J = 7.8 Hz), 7.99 (t, 1H, J = 7.8 Hz), 7.69 (t, 1H, J = 4.4 Hz), 7.54 (d, 1H, J = 6.4 Hz), 5.96 (d, 1H, J = 4.1 Hz), 5.32 (d, 1H, J = 4.2 Hz), 5.00 (s, 1H), 4.22–3.08 (m, 32H), 2.81 (d, 1H), 2.55–2.36 (m, 6H), 2.21–2.17 (m, 2H), 1.82 (q, 1H); MS (MALDI-TOF) m/z for C₅₂H₉₁N₉O₁₅S₂ [M + 2H]⁺ 1136.37, found 1136.75; UV (water) λ_{max} = 343 nm (ϵ = 19625 M⁻¹ cm⁻¹).

RESULTS AND DISCUSSION

Design and Synthesis of a Triple Recognition Agent.

(i) Modeling. As imaginable when viewing the DNA structure, placing the key binding moieties in separate areas would require a linker with significant length and flexibility. Regarding this, we opted for designing the conjugate based on a novel neomycin–Hoechst 33258 conjugate, NH, which maintains a hexaethylene glycol linkage between the two binding moieties. Though NH binding to DNA was shown to be weaker than that of an earlier Neomycin–Hoechst 33258 conjugate (26), we chose to maintain the hexaethylene glycol spacer for NHP for a number of reasons. (a) The linker is long enough to accommodate binding from all three moieties when spaced evenly along the hexaethylene glycol chain (see Figure 2). (b) Direct comparisons can be made with NH to isolate pyrene's effect on DNA binding.

(c) Due to both pyrene and Hoechst binding, the degree of freedom of neomycin for outside solvent interactions is diminished when compared with the neomycin moiety in NH. (d) The commercial availability of (terminal) diamines spaced with di- and triethylene glycols fits conveniently with the synthetic design, not only with NHP but also with NP (see Figure 2). (e) Molecular modeling of NHP indicated a virtually ideal fit with such distances between the binding moieties.

Pyrene is a popular fluorescence tag for studying or identifying biochemical processes in vitro. The intense fluorescence upon exposure to UV allows for sensitive measurements at nanomolar concentrations. Various studies have indicated that pyrene intercalates DNA, yet the strength and selectivity of binding are significantly weaker than those of many well-known DNA intercalators. The ease of its synthetic incorporation into biomolecules largely accounts for its popularity in biochemistry and is the primary reason for its choice in these studies.

In modeling the triple recognition agent, we first docked the three binding moieties in their respective areas: Hoechst in its routine minor groove A/T stretch (as gathered from PDB entry 296d) (51), neomycin in the nearby major groove, and aminopyrene 2 bp above the terminal hydroxyl group of Hoechst 33258. In docking neomycin, the 5'-OH group of the ribose ring was directed toward the minor groove, as would be required if covalently linked to a minor groove binding ligand. Furthermore, the amino position of aminopyrene was directed out of the minor groove, as it would be when conjugated to the Hoechst moiety. After structural minimization, the linker, based on hexaethylene glycol, was constructed to connect the three binding moieties. The structure was further minimized to provide the renderings in Figure 3.

Inspection of the model of NHP with d(CGCAAATTCGCG)₂ clearly indicates a snug fit of Hoechst within the DNA minor groove and significant H-binding sites between neomycin and specific bases, as well as with the strands that line the major groove. A clear increase in the base pair distance is also noticeable in the pyrene intercalation site. The resulting picture is somewhat of a “clamp” on the DNA structure.

(ii) Synthesis of NHP and Control Ligands. The reaction scheme for the preparation of NHP is depicted in Scheme 1. Monotosylation of triethylene glycol using published procedures to provide **5** and subsequent coupling with *p*-cyanophenol using Mitsunobu conditions afforded **6** in good yields. Tosylate substitution with a monoprotected diamine **7** under basic conditions provided intermediate **8**. Reaction of the secondary amine of **8** with pyrene succinimide ester **9** followed by standard coupling with **11** in an ethanol/acetic acid mixture provided the desired Hoechst–pyrene–amine conjugate (HPA, **3**) after subsequent trifluoroacetyl removal (K_2CO_3 , MeOH/H₂O) at the terminal amine (Scheme 1). Reaction of **3** with neomycin isothiocyanate **12** followed by NH-Boc deprotection of coupled product **13** gives the desired triple recognition agent **4** (Scheme 2) as a trifluoroacetate salt.

Traditionally, modifications at the phenol hydroxy group of Hoechst 33258 have been conducted prior to benzimidazole formation. Therefore, functional groups within the linker (at the phenol OH position) must be stable to anhydrous HCl, which is used to convert the *p*-cyano position to a reactive imidate ester for coupling with 1,2-diaminobenzenes to provide the benzimidazole. Conveniently, the pyrene–amide intermediate, formed before benzimidazole formation, is stable to such acidic conditions, as

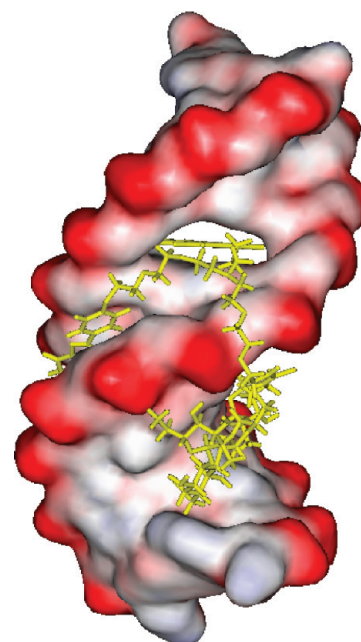


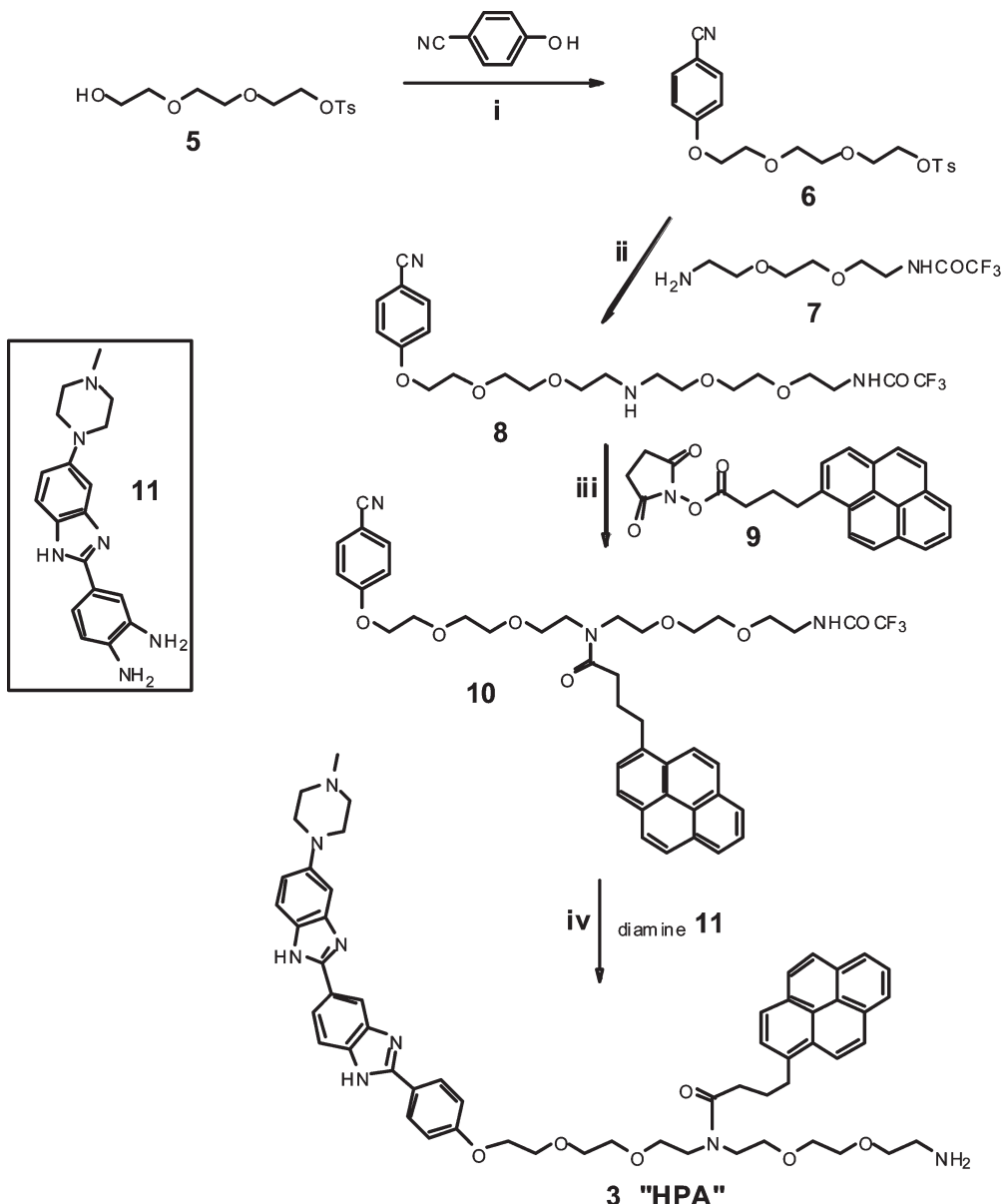
FIGURE 3: Computer model of NHP binding to d(CGCAAATTCGCG)₂. The Hoechst 33258–DNA complex was extracted from PDB entry 296d (51), and further model building was conducted in MacroModel. Energy minimization was conducted before and after the three binding moieties had been linked. The surface potential rendering was created by exporting the PDB file of the minimized structure into WebLabViewer Pro.

well as in a later step where base is used to deprotect the terminal trifluoroacetyl group on the amine.

A novel neomycin–pyrene conjugate (NP) was also prepared for the sake of comparison. NP maintains the identical linkage between neomycin and Hoechst 33258. The synthetic route is outlined in Scheme 3. For its preparation, monoprotected diamine **7** was first reacted with pyrene succinimide ester **9**, which was generated in situ, before trifluoroacetyl deprotection and reaction with neomycin isothiocyanate **12**. N-Boc deprotection of **15** in a CH_2Cl_2/TFA mixture afforded compound **2** (NP) as the trifluoroacetate salt.

(iii) UV Melting and DSC of NHP with the DNA Duplex Suggest Significant Stabilization of the DNA Duplex. The thermal stability of poly(dA)·poly(dT) in the presence of various ligands was first studied by UV melting analysis (Figure 4). In addition to NH, NHP, and Hoechst 33258, additional comparisons were made with a novel neomycin–pyrene conjugate (NP) and Hoechst–pyrene–amine conjugate (HPA), which is a precursor to NHP synthesis. A comparison including HPA allows a direct analysis of neomycin’s (in NHP) effect on DNA stability. A more detailed study of the binding effect by NHP was also achieved with melting experiments consisting of a combination of individual ligands (e.g., NH with aminopyrene in the same solution, and so forth). When compared with those of NH and Hoechst 33258, a noticeable shift in the T_m is lacking for NHP. As indicated in Table 1, ΔT_m values for NH and Hoechst 33258, and combinations containing these ligands (see Figure 4), remain in a similar range ($\Delta T_m = 15^\circ C$), while NHP melts exhibited a less significant shift in T_m ($\Delta T_m = 10^\circ C$). This unanticipated result prompted studies of the NHP–DNA complex by other melting methods, most notably differential scanning calorimetry (DSC). DSC is often used to monitor the dissociation of DNA strands, providing valuable T_m and ΔH values for the association–dissociation process.

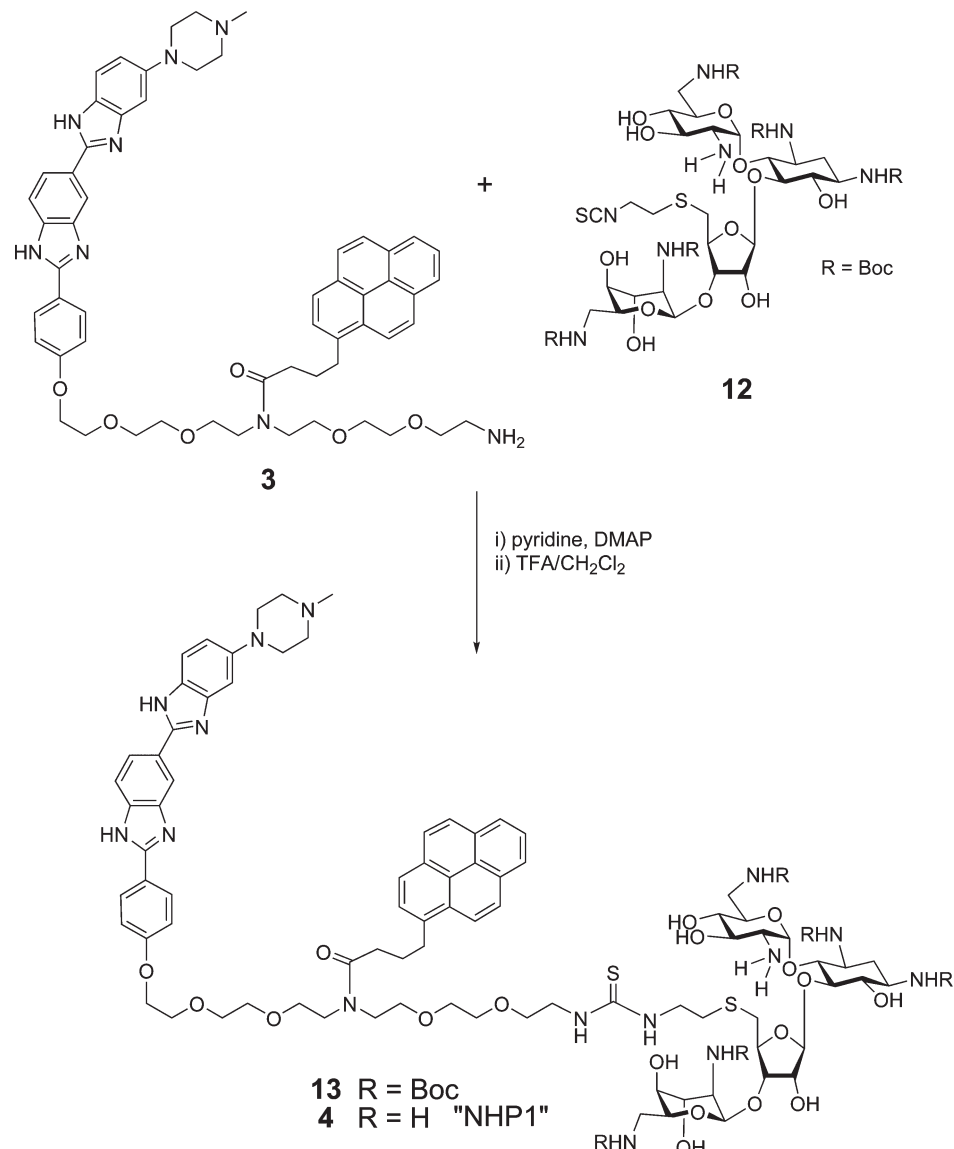
Scheme 1: Preparation of the Hoechst 33258–Pyrene–Amine Conjugate^a



^aReagents and conditions: (i) *p*-cyanophenol, PPh₃, DIAD, dioxane, 78%; (ii) 7, DMF, NaI, 61%; (iii) 9, DMAP, DMF, 65%; (iv) (a) 11, HOAc, EtOH, 41%; (b) K₂CO₃, MeOH, H₂O.

A previous differential scanning calorimetry (DSC) study of a first-generation neomycin–Hoechst 33258 conjugate in a complex with poly(dA)·poly(dT) exhibited an excellent agreement with T_m values determined in UV melting experiments (26). DSC data gathered for the NHP–poly(dA)·poly(dT) complex gave a much different result (Figure 5). The relatively sharp peak corresponding to duplex melting, otherwise present in DNA alone, becomes virtually absent even up to temperatures as high as 110 °C. Intermediate concentrations (less than saturating conditions) indicate melting of unbound DNA (at 72 °C) with one important difference from that of DNA melting with no ligand present: ΔH values at the T_m were significantly lower. It is possible that the T_m for NHP-bound DNA is above that observable in DSC (and UV) experiments. These results, gathered after melting experiments conducted with shorter DNA oligomers (discussed below), struck a chord with what we initially observed, namely, T_m values lower than those anticipated for NHP in UV melting experiments.

It is well-known that pyrene favors the alternating purine-pyrimidine sequence over the nonalternating purine-pyrimidine sequence polymers (54). It was therefore of interest to explore the effect of NHP on the polymer duplex poly(dAdT)₂. UV melting analysis with poly(dAdT)₂ was conducted in a fashion similar to that for poly(dA)·poly(dT)₂. NHP was found to exhibit a significantly larger ΔT_m (16 °C) under the conditions employed versus that found for other ligands (Figure 6), including NP and HPA, further illustrating the contributions of both Hoechst and neomycin toward pyrene binding, a phenomenon not observed for NP and less significant for HPA. Lastly, the direct comparison of NHP with control samples containing a combination of lower-order conjugates and individual ligand (Figure 6 and Table 2), essentially providing all three binders in the DNA sample (e.g., NP–Hoechst 33258), further illustrates the importance of covalently linking the three moieties to achieve optimal recognition. The increase in the ΔT_m of NHP with poly(dAdT)₂ when compared with poly(dA)·poly(dT) can simply be a consequence

Scheme 2: Preparation of Triple Recognition Agent NHP^a

^aReagents and conditions: (i) pyridine, DMAP, 52%; (ii) 1:1 TFA/CH₂Cl₂, quant.

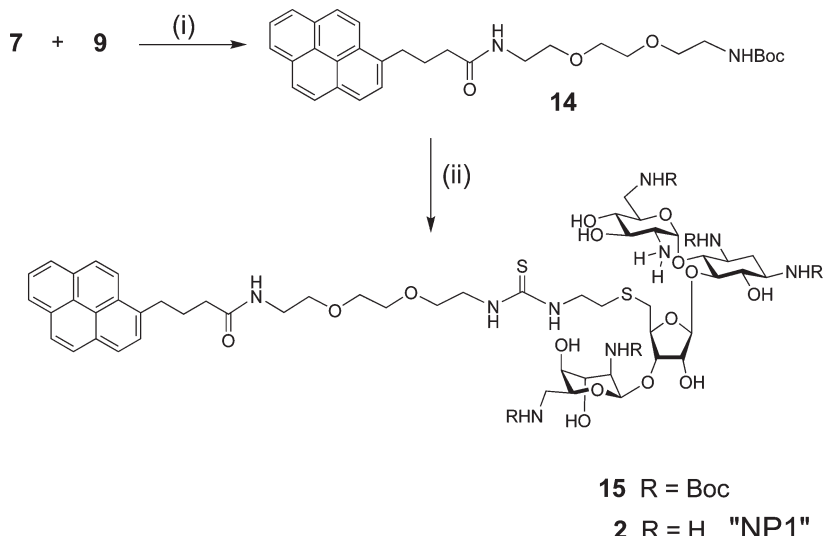
of pyrene's preferential binding to alternating purine-pyrimidine sequences (54).

To test the effect of the conjugates on oligomeric DNA duplex stability, UV melting profiles of dA₂₂·dT₂₂ in the absence and presence of various ligands were gathered in a fashion similar to that used with polymeric DNA (Figure 7). A much more significant and noticeable shift in the T_m for dA₂₂·dT₂₂ with NHP was apparent. When compared with other ligands, such as Hoechst 33258, NH, NP, and HPA, the triple-binding agent NHP was hailed as the strongest stabilizer of this DNA oligomer, with a ΔT_m of 24 °C. A concentration-dependent melting study (Figure 8) illustrates the gradual shift in T_m values as ligand concentrations are increased, with ΔT_m values of up to 32 °C at ligand concentrations of 3 μ M. These results indicate a clear distinction in binding effect for NHP, as solutions containing a combination of individual ligands (NH with aminoypyrene, neomycin with HPA, and NP with Hoechst 33258) exhibited significantly lower T_m values (see Figure 7 and Table 3).

UV melting profiles with d(CGAAATTGCG)₂ with NHP exhibited results similar to those seen with Hoechst 33258, NH,

and HPA (Figure 9). These findings highlight the importance of an extended stretch of A-T base pairs. Furthermore, fluorescence titrations have indicated that the neomycin conjugates reported here prefer A/T stretches of 9 bp. Therefore, the central A₃T₃ region in d(CGAAATTGCG)₂ may be less favorable than DNA oligomers such as dA₂₂·dT₂₂. Melting data (Figures 7 and 8) with such DNA support this. As such, experiments with control ligands as a combination of all three binders, as done with dA₂₂·dT₂₂ and polymeric DNA, exhibited melting profiles similar to those of the individual ligands themselves (Figure 9 and Table 4).

(iv) *Fluorescence Titrations Indicate Significant Binding to Duplex DNA: Poly(dA)·Poly(dT)*. Upon binding to DNA, Hoechst 33258 exhibits a significant fluorescence enhancement (17), due presumably to the loss of solvent exposure upon snugly binding (van der Waals and H-bonding forces) within the DNA groove (55). An established DNA minor groove binder with A/T base pair specificity, Hoechst 33258 was discovered in the early 1990s to display multiple modes of binding to polymeric DNA (56). Binding constants were found to be on the order of

Scheme 3: Synthesis of NP^a

^aReagents and conditions: (i) (a) pyrenebutyric acid, TSTU, DMF, NEt₃, 64%; (b) TFA/CH₂Cl₂, 96%; (ii) (a) neomycin isothiocyanate **12**, pyridine, 62%; (b) 1:1 TFA/CH₂Cl₂, ethanedithiol, 96%.

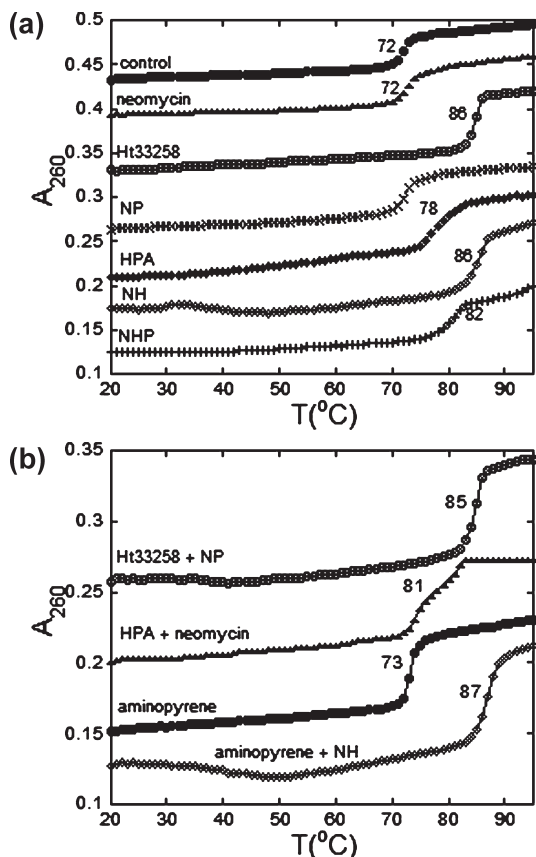


FIGURE 4: UV melting profiles of poly(dA)·poly(dT) with various ligands. Samples of DNA (15 μ M) were mixed with ligand (2 μ M) in buffer [10 mM sodium cacodylate, 0.5 mM EDTA, and 150 mM KCl (pH 7.2)] before being heated at 95 °C for 5 min and slowly annealed to 20 °C before UV analysis at 260 nm from 20 to 95 °C at a heating rate of 0.2 °C/min. T_m values were determined by first-derivative analysis (where clearly discerned) using instrument software or via the midpoint of the transition where broad transitions were observed.

10^8 (M^{-1}) for the sequence-specific interaction (A/T stretch of 4–5 bp). Because of its aggregation at micromolar concentra-

Table 1: T_m Data for Poly(dA)·Poly(dT) Melting in the Presence of the Various Indicated Ligands^a

compound	$T_{m2 \rightarrow 1}$ (°C)	$\Delta T_{m2 \rightarrow 1}$ (°C)
none	72	0
neomycin	72	0
Hoechst 33258	86	14
aminopyrene	73	1
NP	78	6
NH	86	14
HPA	78	6
NHP	82	10
NH–aminopyrene	87	15
HPA–neomycin	81	9
NP–Hoechst 33258	85	13

^aSamples of DNA (15 μ M) were mixed with ligand (2 μ M) in buffer [10 mM sodium cacodylate, 0.5 mM EDTA, and 150 mM KCl (pH 7.2)] before being heated at 95 °C for 5 min and slowly annealed to 20 °C before UV analysis at 260 nm from 20 to 95 °C at a heating rate of 0.2 °C/min. T_m values were determined by first-derivative analysis (where clearly discerned) using instrument software or via the midpoint of the transition where broad transitions were observed.

tions (56), fluorescence techniques have been primarily utilized for probing Hoechst 33258 binding. Furthermore, because of its tight binding to DNA, the requirement for experimental substrate concentrations on the order of $1/K_b$ for gathering appropriate binding isotherms eliminates the utility of other spectroscopic techniques due to weak signal detection.

Fluorescence titrations of the novel conjugates, as well as Hoechst 33258, with poly(dA)·poly(dT) were conducted in a fashion similar to that reported previously (56–58). The experiments typically consisted of titrations of a fixed ligand concentration (10 nM) with a concentrated DNA sample, with fluorescence emission scans gathered at each ligand:DNA ratio after the appropriate equilibration time. The resulting binding isotherm could then be fit to a theoretical model, providing binding constants (K_b) for the respective ligands. Because of multiple modes of binding of Hoechst 33258 with polymeric DNA, with ligand:phosphate stoichiometries of up to 2:1 (56), titrations of low (nanomolar) ligand concentrations with DNA to

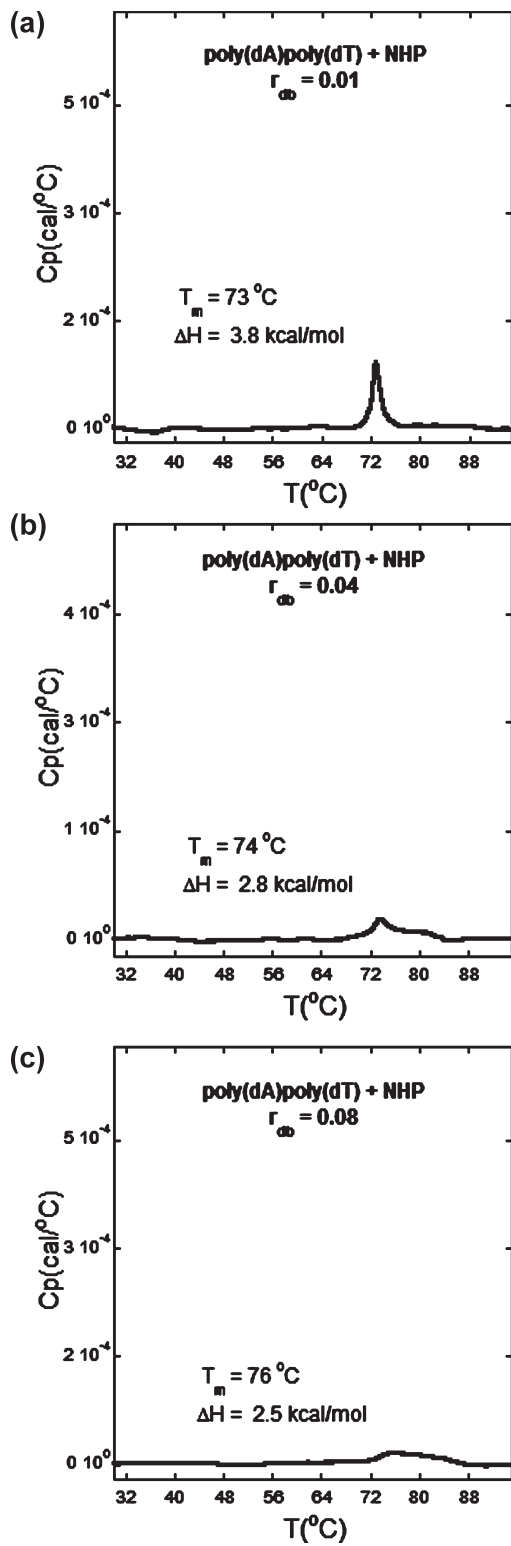


FIGURE 5: DSC profiles of 100 μ M poly(dA) · poly(dT) with increasing concentrations of NHP: (a) 1 μ M NHP, (b) 4 μ M NHP, and (c) 8 μ M NHP. Buffer conditions were identical to those in UV melting experiments. Samples were heated at a rate of 0.5 $^{\circ}$ C/min. Values for T_m and ΔH were determined using Origin version 7.0 provided with the instrument.

yield low ligand:DNA ratios were conducted to simulate nearly independent site binding characteristics. In this approach, the low ligand:DNA ratio exhibits a fluorescence signal corresponding to a sequence-specific binding event. Thus, the resulting binding curve can be fit using an independent site model for tight binding,

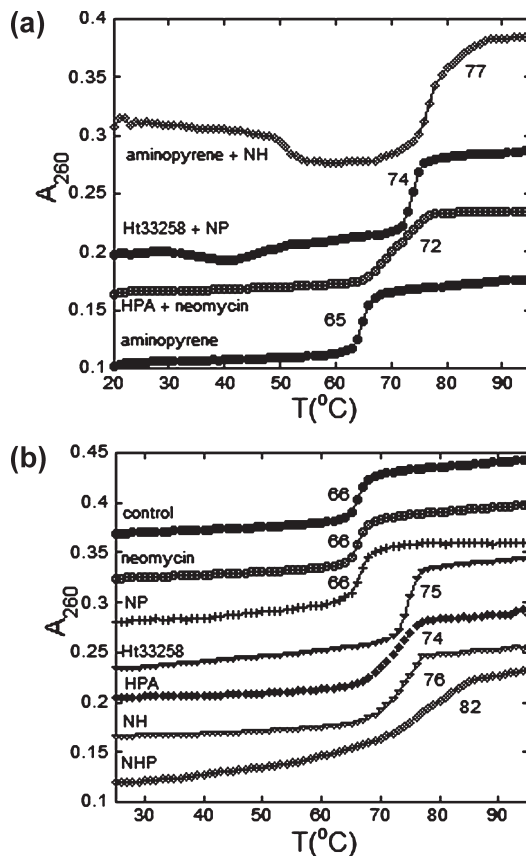


FIGURE 6: UV melting profiles of poly(dAdT)₂ with various ligands. Samples of DNA (20 μ M) were mixed with ligand (3 μ M) in buffer [10 mM sodium cacodylate, 0.5 mM EDTA, and 150 mM KCl (pH 7.2)] before being heated at 95 $^{\circ}$ C for 5 min and slowly annealed to 20 $^{\circ}$ C before UV analysis at 260 nm from 20 to 95 $^{\circ}$ C at a heating rate of 0.2 $^{\circ}$ C/min. T_m values were determined by first-derivative analysis (where clearly discerned) using instrument software or via the midpoint of the transition where broad transitions were observed.

Table 2: T_m Data for poly(dAdT)₂ Melting in the Presence of Various Indicated Ligands^a

compound	$T_{m2 \rightarrow 1}$	$\Delta T_{m2 \rightarrow 1}$
none	66	0
neomycin	66	0
Hoechst 33258	75	9
aminopyrene	65	-1
NP	66	0
NH	76	10
HPA	74	8
NHP	82	16
NH–aminopyrene	77	11
HPA–neomycin	72	6
NP–Hoechst 33258	74	8

^aSamples of DNA (20 μ M) were mixed with ligand (3 μ M) in buffer [10 mM sodium cacodylate, 0.5 mM EDTA, and 150 mM KCl (pH 7.2)] before being heated at 95 $^{\circ}$ C for 5 min and slowly annealed to 20 $^{\circ}$ C before UV analysis at 260 nm from 20 to 95 $^{\circ}$ C at a heating rate of 0.2 $^{\circ}$ C/min. T_m values were determined by first-derivative analysis (where clearly discerned) using instrument software or via the midpoint of the transition where broad transitions were observed.

provided the binding site size, N , is known. Once N is known, the DNA (base pairs) concentrations at each titration point can be divided by N to provide the binding site size that is necessary for the determination of binding constant data.

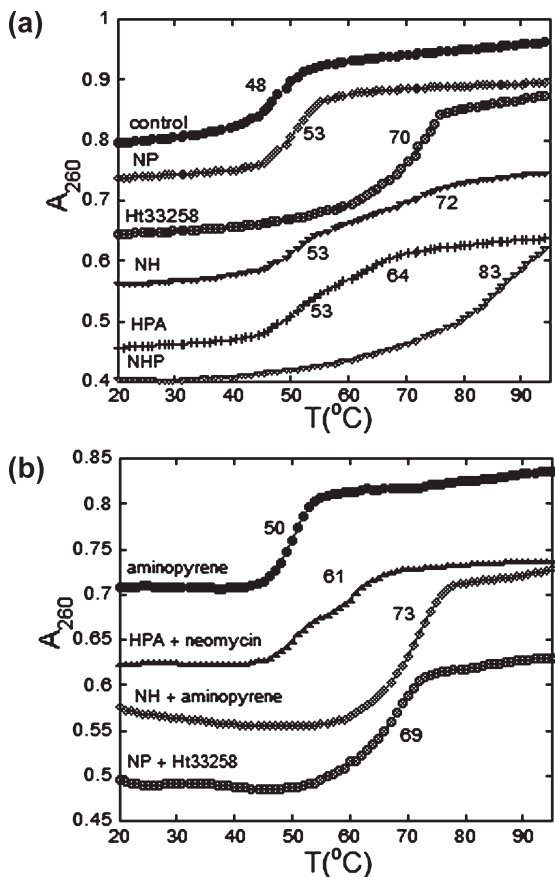


FIGURE 7: UV melting profiles of $dA_{22} \cdot dT_{22}$ with various ligands. Samples of DNA ($1 \mu\text{M}$ in duplex) were mixed with ligand ($3 \mu\text{M}$) in buffer [10 mM sodium cacodylate, 0.5 mM EDTA, and 150 mM KCl (pH 6.8)] before being heated at 95°C for 5 min and slowly annealed to 20°C before UV analysis at 260 nm from 20 to 95°C at a heating rate of $0.2^\circ\text{C}/\text{min}$. T_m values were determined by first-derivative analysis (where clearly discerned) using instrument software or via the midpoint of the transition where broad transitions were observed.

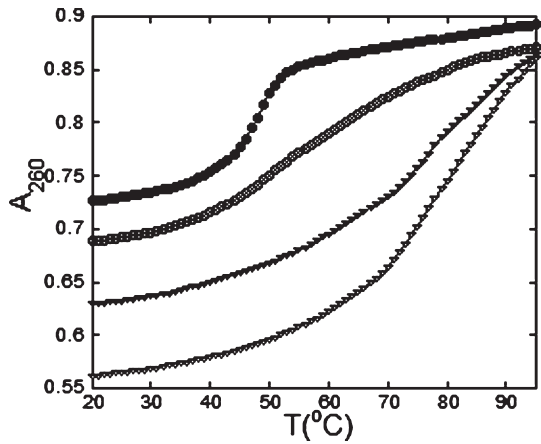


FIGURE 8: UV melting profiles of $dA_{22} \cdot dT_{22}$ with NHP. Samples of DNA ($1 \mu\text{M}$ in duplex) were mixed with ligand ($0, 1, 2$, and $3 \mu\text{M}$ from left to right) in buffer [10 mM sodium cacodylate, 0.5 mM EDTA, and 150 mM KCl (pH 6.8)] before being heated at 95°C for 5 min and slowly annealed to 20°C before UV analysis at 260 nm from 20 to 95°C at a heating rate of $0.2^\circ\text{C}/\text{min}$. T_m values were determined by first-derivative analysis (where clearly discerned) using instrument software or via the midpoint of the transition where broad transitions were observed.

In our experiments with Hoechst 33258, an N value of 10 was used, as established in the literature (59). Separate experiments, in

Table 3: T_m Data for $dA_{22} \cdot dT_{22}$ Melting in the Presence of Various Indicated Ligands^a

ligand	$T_{m2 \rightarrow 1}$	$\Delta T_{m2 \rightarrow 1}$
none	48	0
neomycin	48	0
Hoechst 33258	70	22
aminopyrene	50	2
NP	53	5
NH	72 ^b	24 ^b
HPA	64 ^b	16 ^b
NHP	83	35
NH–aminopyrene	73	25
HPA–neomycin	61 ^b	13 ^b
NP–Hoechst 33258	69	21

^aSamples of DNA ($1 \mu\text{M}$ in duplex) were mixed with ligand ($3 \mu\text{M}$) in buffer [10 mM sodium cacodylate, 0.5 mM EDTA, and 150 mM KCl (pH 6.8)] before being heated at 95°C for 5 min and slowly annealed to 20°C before UV analysis at 260 nm from 20 to 95°C at a heating rate of $0.2^\circ\text{C}/\text{min}$. T_m values were determined by first-derivative analysis (where clearly discerned) using instrument software or via the midpoint of the transition where broad transitions were observed. ^bFor compounds **1** and **3**, biphasic transitions were observed (at an unbound T_m of 51 and the indicated T_m).

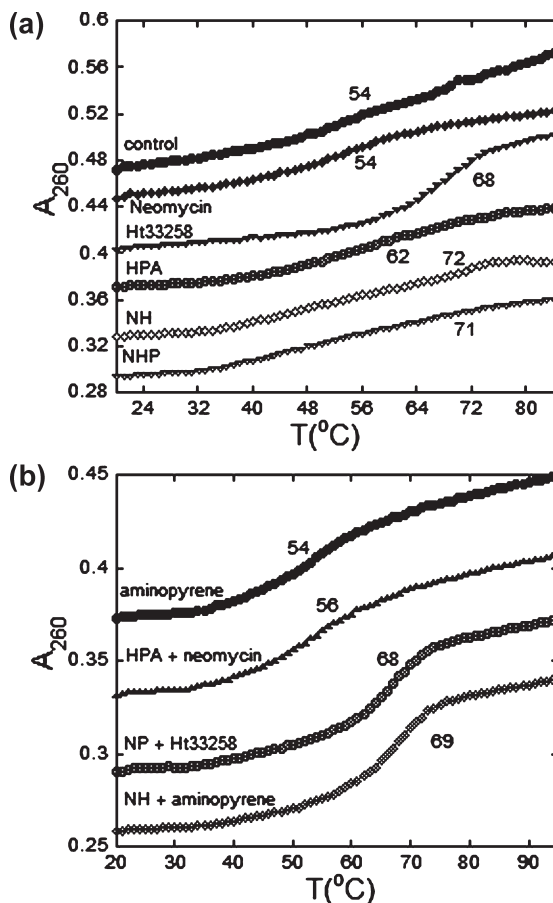


FIGURE 9: UV melting profiles of $d(\text{CGAAATTGCG})_2$ with various ligands. Samples of DNA ($1 \mu\text{M}$ in duplex) were mixed with ligand ($1 \mu\text{M}$) in BPES buffer [6 mM Na_2HPO_4 , 2 mM NaHPO_4 , 1 mM EDTA, and 185 mM NaCl (pH 7.0)] before being heated at 95°C for 5 min and slowly annealed to 20°C before UV analysis at 260 nm from 20 to 95°C at a heating rate of $0.2^\circ\text{C}/\text{min}$. T_m values were determined by first-derivative analysis (where clearly discerned) using instrument software or via the midpoint of the transition where broad transitions were observed.

which a constant DNA concentration was titrated with concentrated ligand to provide values of n (number of base pairs per

Table 4: T_m Data for d(CGCAAATTCGCG)₂ Melting in the Presence of the Indicated Ligands^a

compound	$T_{m2 \rightarrow 1}$	$\Delta T_{m2 \rightarrow 1}$
none	54	0
neomycin	54	0
Hoechst 33258	68	14
aminopyrene	54	0
NH	72	18
HPA	62	8
NHP	71	17
NH–aminopyrene	69	15
HPA–neomycin	56	2
NP–Hoechst 33258	68	14

^aSamples containing DNA (1 μ M in duplex) and ligand (1 μ M) in buffer [6 mM Na₂HPO₄, 2 mM NaHPO₄, 1 mM EDTA, and 185 mM NaCl (pH 7.0)] were heated at 95 °C for 5 min before being slowly annealed to room temperature before UV melting analysis (monitored at 260 nm from 20 to 95 °C at a heating rate of 0.2 °C/min.). T_m values were determined by first-derivative analysis (where clearly discerned) using instrument software or via the midpoint of the transition where broad transitions were observed.

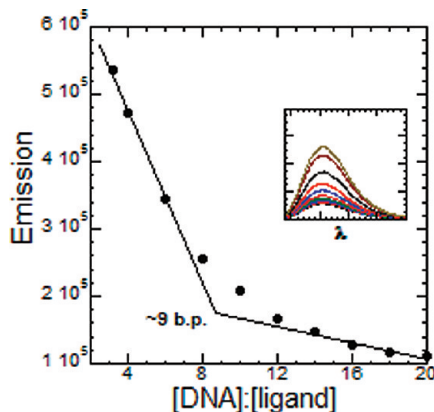


FIGURE 10: Fluorescence titration of NHP into poly(dA)·poly(dT). Small aliquots of concentrated ligand were added to DNA (2 μ M) before fluorescence analysis (excitation at 345 nm, emission scanning from 370 to 600 at 1 nm/s; 4 nm slit width; $T = 25$ °C). Buffer: 10 mM sodium cacodylate, 0.5 mM EDTA, and 150 mM KCl (pH 7.2).

ligand), were conducted and used for determining N . It has been shown that $N = 2(n - 1)$ (60). As indicated by a break in the fluorescence signal when plotted against varying DNA (base pairs):ligand ratios, n values of 9 for both conjugates NH and NHP were observed (Figures 10 and 11). This value is reasonable due to the presence of the neomycin moiety, which likely extends beyond the Hoechst binding site and/or perturbs the DNA environment to exclude binding further down the DNA lattice.

In the case for NHP, one would anticipate the binding site to be larger than NH, due to pyrene intercalation. However, the freedom of the hexaethylene glycol–neomycin arm of NH potentially extends further than that in NHP, due to a “locking in” of the Hoechst and pyrene moieties to their preferred binding areas, restricting the reach of the neomycin arm relative to that in NH.

Binding curves depicting the ligand–DNA interaction are represented in Figures 12–14. For all ligands, as with NHP, fluorescence enhancement with an increasing DNA concentration was observed. All curves, as suggested above, could be successfully curve fit to provide binding constants for each ligand. Resulting binding data are listed in Table 5. Similar to that reported previously (57), Hoechst 33258 binding is approximately $1 \times 10^8 \text{ M}^{-1}$. Binding of the neomycin–Hoechst 33258

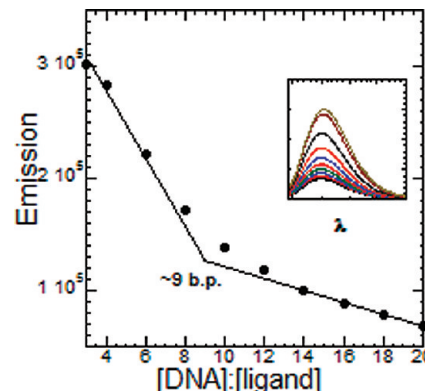


FIGURE 11: Fluorescence titration of NH into poly(dA)·poly(dT). Small aliquots of concentrated ligand were added to DNA (2 μ M) before fluorescence analysis (excitation at 345 nm, emission scanning from 370 to 600 at 1 nm/s; 4 nm slit width; $T = 25$ °C). Buffer: 10 mM sodium cacodylate, 0.5 mM EDTA, and 150 mM KCl (pH 7.2).

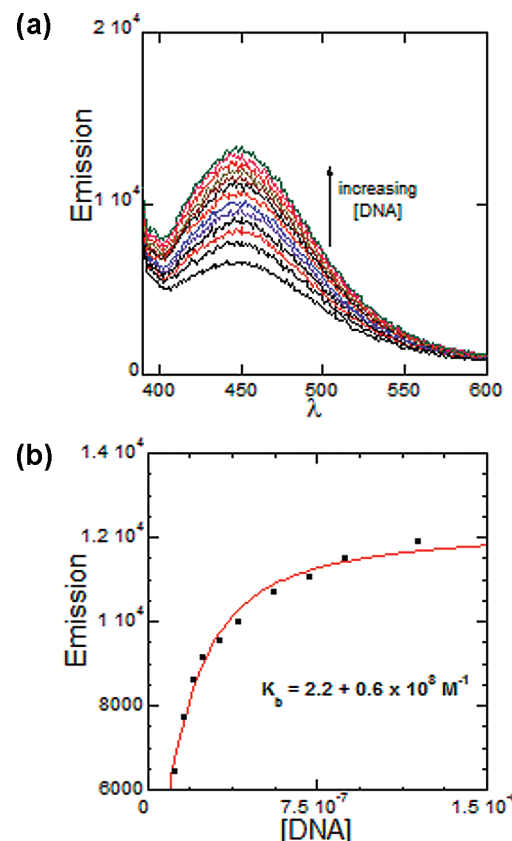


FIGURE 12: Fluorescence-detected binding of NHP to poly(dA)·poly(dT). Small aliquots (1.5–20 μ L) of DNA (200 μ M bp⁻¹) were added to a solution of ligand (2.5 mL of a 10 nM solution) before fluorescence analysis (excitation at 345 nm, emission scanning from 370 to 600 at 1 nm/s; 4 nm slit width; $T = 25$ °C). Buffer: 10 mM sodium cacodylate, 0.5 mM EDTA, and 150 mM KCl (pH 7.2).

conjugate possessing the hexaethylene glycol linker (NH) exhibited markedly less binding affinity ($K_b = 0.3 \times 10^8 \text{ M}^{-1}$) than the other conjugates, including Hoechst 33258. The triple recognition agent, NHP, displayed the highest binding affinity ($2.2 \times 10^8 \text{ M}^{-1}$) of all the ligands, including NH ($1.6 \times 10^8 \text{ M}^{-1}$), which has been shown to significantly stabilize poly(dA)·poly(dT) over Hoechst 33258. We therefore believe that the affinity of NHP for poly(dA)·poly(dT) can be partially attributed to pyrene intercalation.

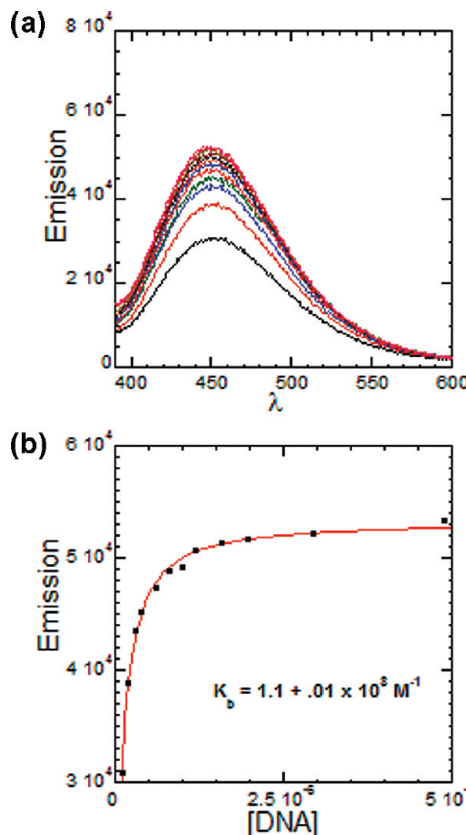


FIGURE 13: Fluorescence-detected binding of poly(dA)·poly(dT) with Hoechst 33258. Small aliquots (1–20 μL) of DNA ($200 \mu\text{M bp}^{-1}$) were added to a solution of ligand (2 mL of a 10 nM solution) before fluorescence analysis (excitation at 338 nm, emission scanning from 390 to 600 at 1 nm/s; 4 nm slit width; $T = 25^\circ\text{C}$). Buffer: 10 mM sodium cacodylate, 0.5 mM EDTA, and 150 mM KCl (pH 7.2).

$d(\text{CGCAAATTGCG})_2$. Fluorescence titrations of the novel ligands were also conducted with $d(\text{CGCAAATTGCG})_2$, an oligomer possessing a single site for Hoechst 33258 binding. Like reported observations (56), the binding of Hoechst 33258 and similar ligands (61) was found to exhibit a 1:1 stoichiometry by way of fluorescence mixing curves [Job plots (Supporting Information)]. With a 1:1 stoichiometry, the fluorescence-detected binding isotherms, the resulting titrations could be fit to an independent, single-site model for tight binding to provide binding constants for each ligand.

Figures 15–17 depict the binding isotherms recorded for the conjugates with $d(\text{CGCAAATTGCG})_2$. Surprisingly, the binding of all the neomycin conjugates was found to be significantly weaker than that found with Hoechst 33258 ($1.8 \times 10^8 \text{ M}^{-1}$; comparable with reported values of $3 \times 10^8 \text{ M}^{-1}$) (62). Clearly, neomycin has little preference for this A-tract duplex. Neomycin dimers on the other hand have recently been shown to prefer A/T rich duplexes (63). The larger binding site size of the ligand, absent in this duplex, also contributes to the lower affinity. Enhanced binding (vs that of Hoechst 33258) is observed in extended A/T stretches [poly(dA)·poly(dT)], suggesting neomycin's role in the binding event. What is absolutely clear, however, is the effect of pyrene intercalation when comparing NH to NHP. There is a 7-fold increase in affinity observed upon going from NH to NHP for the polynucleotide as well as the oligomer (Table 5).

(i) *Breaking up the A/T Stretch: Specificity of Hoechst Binding in the NHP Conjugate.* To improve our knowledge of the design of dual binding ligands, we found it necessary to probe

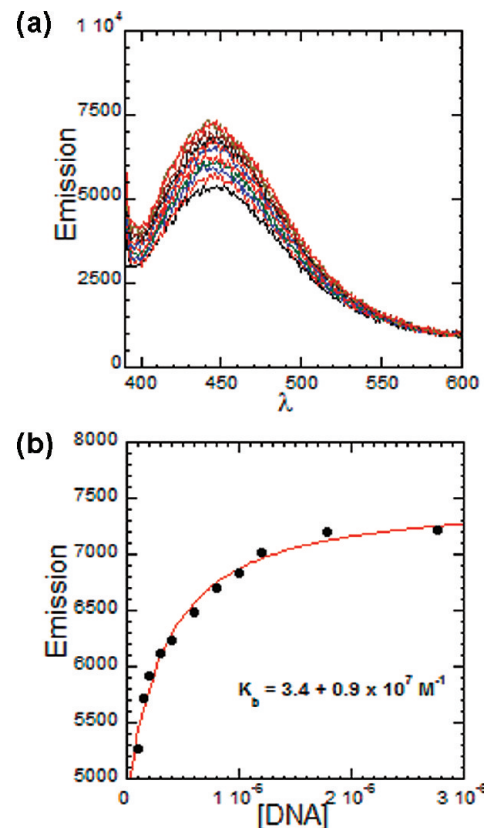


FIGURE 14: Fluorescence-detected binding of poly(dA)·poly(dT) and NH. Small aliquots (1–20 μL) of DNA ($200 \mu\text{M bp}^{-1}$) were added to a solution of ligand (2 mL of a 10 nM solution) before fluorescence analysis (excitation at 338 nm, emission scanning from 390 to 600 at 1 nm/s; 4 nm slit width; $T = 25^\circ\text{C}$). Buffer: 10 mM sodium cacodylate, 0.5 mM EDTA, and 150 mM KCl (pH 7.2).

Table 5: Binding Data for Studied Ligands^a

conjugate	$\text{poly(dA)} \cdot \text{poly(dT)} K (\times 10^7 \text{ M}^{-1})$	$\text{A}_3\text{T}_3 K (\times 10^7 \text{ M}^{-1})$
NH	3.4 ± 0.9	0.5 ± 0.3
NHP	22 ± 0.6	3.5 ± 1.2

^aValues for K_b were determined by nonlinear curve fitting of fluorescence titrations according to an independent site model using conditions similar to those reported. Values for N (binding site size) were either used as reported (Ht33258) or determined experimentally (see Methods).

the affinity of Hoechst 33258, and the neomycin conjugates for sequences in which a GC junction interrupts the A_nT_n stretch. Hoechst 33258 has been shown to bind A/T stretches from 4 to 6 bp in length. Introduction of G/C base pairs has also been shown to significantly weaken the binding of Hoechst 33258. Therefore, studying a sequence with a GC junction can provide deeper insight into neomycin's role in binding. For example, does binding enhancement by neomycin perturb the sequence specificity of Hoechst? Furthermore, what effects do pyrene and neomycin conjugation have on Hoechst binding a G-C base pair breaking up the A-tract? Thus, we chose to study DNA duplex $d(\text{CGCAAGCTTGCG})_2$.

Fluorescence titration experiments with $d(\text{CGCAAGCTTGCG})_2$ with Hoechst 33258 and NHP were conducted like those experiments with the central A_3T_3 stretch (Figure 18). In the case of Hoechst 33258, the observed K_b was significantly lower than what was observed for $d(\text{CGCAAATTGCG})_2$. The binding is nearly 1000-fold weaker ($3.7 \times 10^5 \text{ M}^{-1}$), validating previous

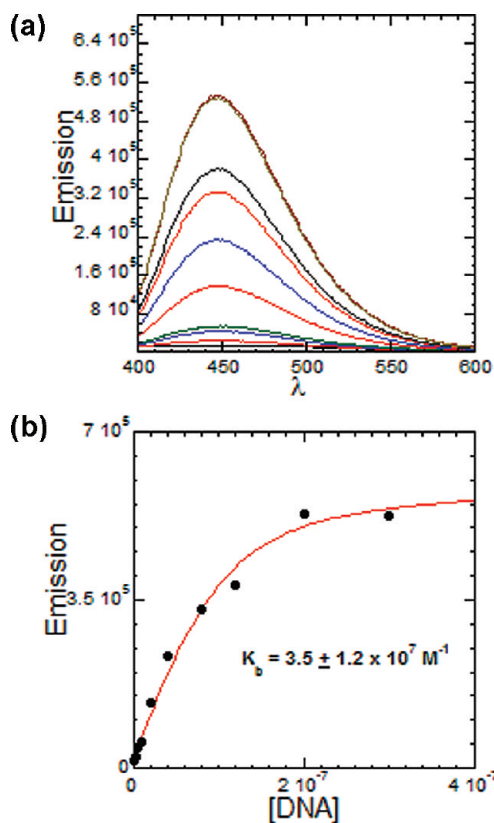


FIGURE 15: Fluorescence-detected binding of NHP with d(CGCA-AATTTGCG)₂. Samples of ligand (100 nM in 2 mL) mixed with varying concentrations of DNA were analyzed for fluorescence emission over a 390–600 nm range. Conditions: $\lambda_{\text{exc}} = 345 \text{ nm}$; 6 nm slits; $T = 20^\circ \text{C}$. Buffer: BPES [6 mM Na₂HPO₄, 2 mM NaH₂PO₄, 180 mM NaCl, and 2 mM Na₂EDTA (pH 7.0)].

accounts which indicated a strong binding preference of Hoechst ligands for A_nT_n regions of DNA. Comparison with HPA was difficult due to the solubility of the ligand under the conditions used. However, experiments with NHP indicated a more favorable binding interaction with this duplex, stabilizing it nearly 10-fold more than Hoechst 33258. Therefore, pyrene and neomycin both play a clear role in binding to d(CGCAAGCTT-GCG)₂ and force Hoechst to bind within the groove (as indicated by the observed fluorescence enhancement in these experiments) with a greater impact than Hoechst 33258 alone.

(ii) *Circular Dichroism of Poly(dA)·Poly(dT) in the Presence of NHP Indicates Considerable Conformational Changes in both DNA and the Hoechst–Pyrene Regions.* We utilized circular dichroism (CD) spectroscopy to study the changes, if any, in the poly(dA)·poly(dT) structure as well as in the Hoechst moiety of the conjugate. Numerous reports have explained binding-induced chirality of Hoechst 33258 by DNA, typically indicated by a change in the CD signal at the λ_{max} of Hoechst 33258 UV absorbance (64, 65). In our studies, we conducted titrations of ligand into a solution of DNA, with CD scans of the solution taken after appropriate equilibration times between ligand additions. The resulting scans were overlaid to compare the CD spectra at different ligand:DNA ratios (Figures 19–22). We found that there is a significant change in the CD signal in the poly(dA)·poly(dT) region, which is represented by a negative band at 248 nm and a positive band at 260 nm. Also, in the region of 360 nm, there is an increasingly positive CD signal as ligand:DNA ratios are increased, indicative of complexation of Hoechst with the DNA. Additionally, peaks

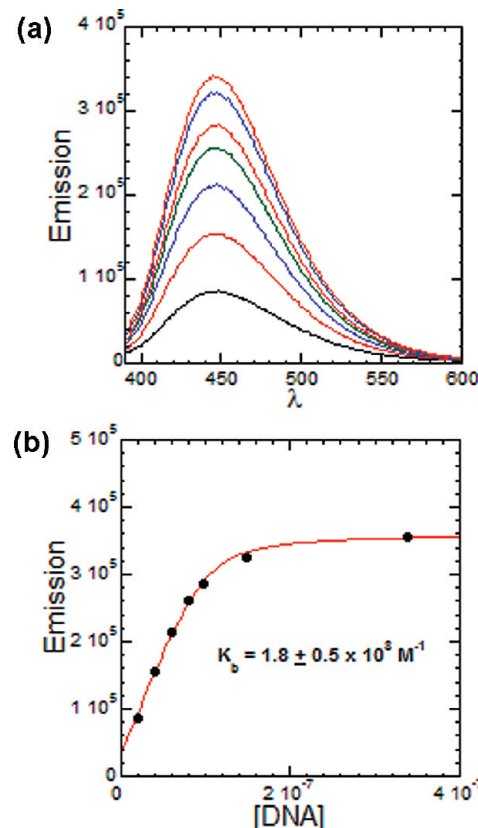


FIGURE 16: Fluorescence-detected binding of Hoechst 33258 with d(CGCAAATTGCG)₂. Samples of ligand (100 nM in 2 mL) mixed with varying concentrations of DNA were analyzed for fluorescence emission over a 390–600 nm range. Conditions: $\lambda_{\text{exc}} = 338 \text{ nm}$; 4 nm slits; $T = 20^\circ \text{C}$. Buffer: BPES [6 mM Na₂HPO₄, 2 mM NaH₂PO₄, 180 mM NaCl, and 2 mM Na₂EDTA (pH 7.0)].

characteristic of pyrene absorption appear to overlap (270–400 nm, likely due to a $\pi-\pi^*$ absorption of the pyrene moiety) with the Hoechst region. Since asymmetry is induced in both chromophores upon binding to DNA, these data support the hypothesis that both Hoechst 33258 and pyrene regions of NHP are interacting with the DNA.

Pyrene binding to poly(dA)·poly(dT) has been shown to occur in an “external”, nonintercalative fashion that is characterized by little change in T_m , viscosity, or circular dichroism in pyrene’s absorption region (54, 66). Our observations with NHP in the presence of poly(dA)·poly(dT) suggest an intercalative binding mode similar to that of poly(dAdT)₂ (66, 67). Therefore it is likely that a combination of conformational restrictions in NHP and the resulting unwinding of the duplex by dual groove binding of neomycin and Hoechst 33258 designates pyrene to an intercalative binding mode. Virtually no change in the CD spectrum of the DNA region (200–260 nm) suggests that DNA conformation is relatively unperturbed upon ligand binding.

(iii) *Viscometric Titrations Suggest Intercalation by the Pyrene Moiety.* The experimental results at this point led us to propose a multivalent recognition process for NHP. Equilibrium binding data indicated an enhanced binding over both NH (**1**) (which contains a linker nearly identical to NHP) and NH' (a conjugate with a shorter linker than NH), previously shown to significantly bind DNA better than Hoechst 33258 (26). Circular dichroism results (Figure 22) suggested Hoechst and pyrene interaction. We further chose to confirm pyrene intercalation using viscometric analysis.

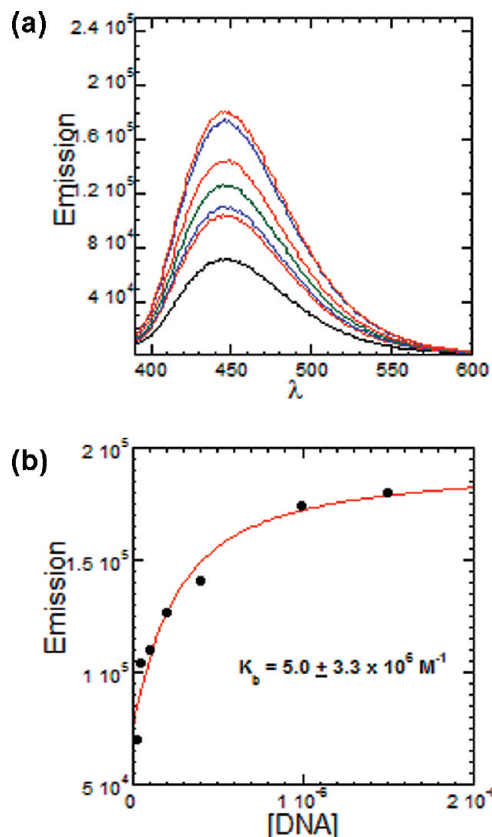


FIGURE 17: Fluorescence-detected binding of d(CGCAAATTTG-CG)₂ with NH. Individual samples of ligand (100 nM in 2 mL) mixed with varying concentrations of DNA were prepared immediately after quantitation of both stock ligand and DNA solutions. After sufficient mixing of solutions and equilibration time (30 min), each sample was analyzed for fluorescence emission over the 390–600 nm range. Conditions: $\lambda_{\text{exc}} = 338$ nm; 4 nm slits; $T = 20$ °C. Buffer: BPES [6 mM Na₂HPO₄, 2 mM NaH₂PO₄, 180 mM NaCl, and 2 mM Na₂EDTA (pH 7.0)].

Viscometry has long been utilized for investigating ligand–substrate binding modes, particularly to confirm intercalation events. Intercalation of nucleic acids results in an increase in the helical length, because of space displacement between the base pairs by the ligand. Nucleic acids of appropriate length are rodlike, so an increase in helical length results in an increase in solution viscosity (68). Thus, we conducted viscometric titrations of neomycin, Hoechst 33258, NH, and NHP with poly(dA)·poly(dT) (Figure 23). The results were, at first, unanticipated since groove binding molecules such as Hoechst 33258 with DNA display little change in intrinsic solution viscosity. In all cases except Hoechst 33258, the DNA solution viscosity decreased when ligand was added. The most marked decrease was with NH, whereas that with NHP was clearly higher. Similar to that observed before (69, 70), the decrease in viscosity can be attributed to groove binding, which, in contrast to intercalation, can shorten the helix by compaction. This compacting of DNA is clearly a result of neomycin interaction, further corroborating neomycin's role in the multirecognition process. However, the binding degree of NHP can be extended further.

By subtracting the results of NH–DNA binding from NHP–DNA binding in the viscosity experiments, we can ascertain the effect of the pyrene moiety in NHP on the DNA. A closer look, by this consideration, clears the view somewhat. By overlaying the subtracted data [NHP minus NH (Figure 24)], we observe a clear resemblance to theoretical intercalation for the

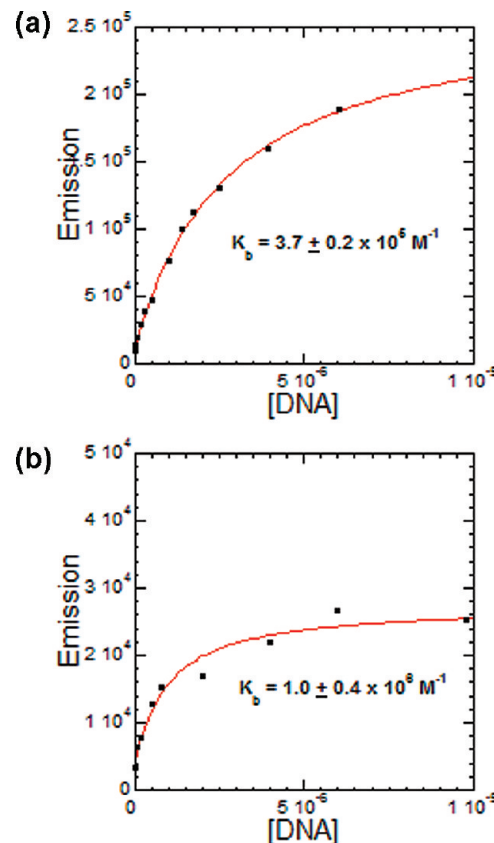


FIGURE 18: Fluorescence-detected binding curves of d(CGCAAG-CTTGC)₂ binding to Hoechst 33258 (left) and NHP (right). Individual samples of ligand (100 nM in 2 mL) mixed with varying concentrations of DNA were prepared immediately after quantitation of both stock ligand and DNA solutions. After sufficient mixing of solutions and equilibration time (30 min), each sample was analyzed for fluorescence emission over the 390–600 nm range. Conditions: $\lambda_{\text{exc}} = 338$ nm; 4 nm slits; $T = 20$ °C. Buffer: BPES [6 mM Na₂HPO₄, 2 mM NaH₂PO₄, 180 mM NaCl, and 2 mM Na₂EDTA (pH 7.0)].

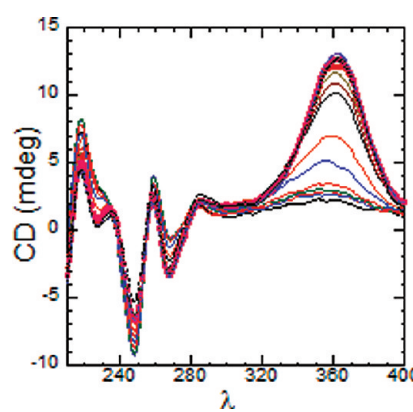


FIGURE 19: CD scans of poly(dA)·poly(dT) with increasing concentrations of Hoechst 33258. Samples of DNA (40 mM) were scanned from 400 to 210 nm after serial additions of concentrated ligand with stirring. Peaks around 360 nm correspond to ligand–DNA complexation. Buffer: 10 mM sodium cacodylate, 0.5 mM EDTA, and 150 mM KCl (pH 7.2). $T = 20$ °C.

pyrene moiety in NHP. Therefore, there is a clear correlation of NHP with intercalation of poly(dA)·poly(dT). The slightly lower value can be attributed to intercalation occurring less periodically within the DNA lattice due to the large binding site size (vs a simple intercalator that would intercalate every 3 bp).

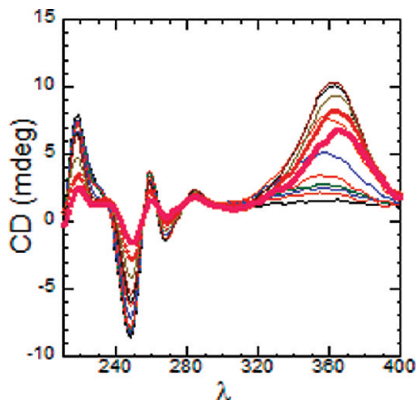


FIGURE 20: CD scans of poly(dA)·poly(dT) with increasing concentrations of NH. Samples of DNA (40 mM) were scanned from 400 to 210 nm after serial additions of concentrated ligand with stirring. Peaks around 360 nm correspond to ligand–DNA complexation. Buffer: 10 mM sodium cacodylate, 0.5 mM EDTA, and 150 mM KCl (pH 7.2). $T = 20^\circ\text{C}$.

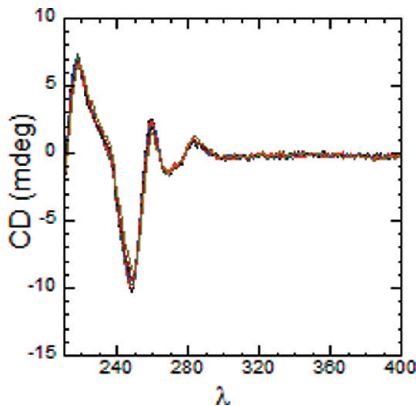


FIGURE 21: CD scans of poly(dA)·poly(dT) with increasing concentrations of NP. Samples of DNA (40 mM) were scanned from 400 to 210 nm after serial additions of concentrated ligand with stirring. Buffer: 10 mM sodium cacodylate, 0.5 mM EDTA, and 150 mM KCl (pH 7.2). $T = 20^\circ\text{C}$.

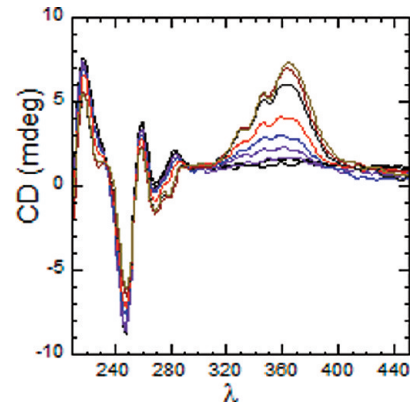


FIGURE 22: Circular dichroism of poly(dA)·poly(dT) complexed with NHP. A solution of DNA (30 μM) was titrated with small aliquots of concentrated ligand (200 μM) before equilibration and scanning from 450 to 210 nm. Peaks around 360 nm correspond to ligand–DNA complexation. Solutions were in 10 mM sodium cacodylate, 0.5 mM EDTA, and 150 mM KCl (pH 7.2). The temperature was ambient.

Furthermore, the mere observation of viscosity decrease, as seen in other accounts, confirms neomycin binding. Lastly, multiple spectroscopic experiments have conveyed the Hoechst moiety's

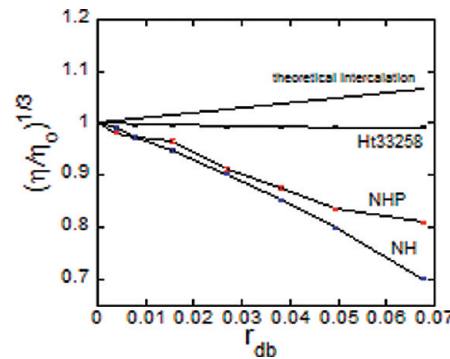


FIGURE 23: Viscometric analysis of poly(dA)·poly(dT) with various ligands. DNA solutions (100 μM) were titrated with the respective drug (200 μM), and corresponding flow times were recorded in triplicate with a deviation of <0.1 s. Error bars are indicated for each titration point. Buffer: 10 mM sodium cacodylate, 0.5 mM EDTA, 150 mM KCl, and 1 mM MgCl₂ (pH 7.2). $T = 27 \pm 0.05^\circ\text{C}$.

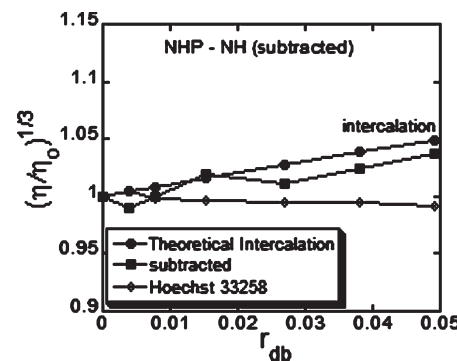


FIGURE 24: Subtracted viscosity data to convey the effect of pyrene on solution viscosity. DNA solutions (100 μM) were titrated with the respective drug (200 μM), and corresponding flow times were recorded in triplicate with a deviation of <0.1 s. Buffer: 10 mM sodium cacodylate, 0.5 mM EDTA, 150 mM KCl, and 1 mM MgCl₂ (pH 7.2). $T = 27 \pm 0.05^\circ\text{C}$.

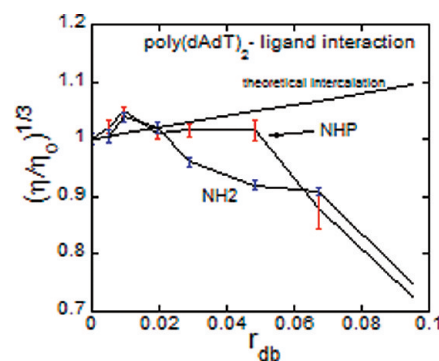


FIGURE 25: Viscometric analysis of poly(dAdT)₂ with various ligands. DNA solutions (100 μM) were titrated with the respective drug (200 μM), and corresponding flow times were recorded in triplicate. Error bars are indicated for each titration point. Buffer: 10 mM sodium cacodylate, 0.5 mM EDTA, 150 mM KCl, and 1 mM MgCl₂ (pH 7.2). $T = 27 \pm 0.05^\circ\text{C}$.

presence in DNA binding. Thus, convincing evidence, from a combination of analytical techniques, gives strong candidacy for a DNA triple recognition agent in NHP.

Further viscometric analysis of alternating A/T base pair intercalation was done using poly(dAdT)₂. Unlike that seen with poly(dA)·poly(dT), the viscosity of poly(dAdT)₂ solutions was found to increase upon titration of NHP (Figure 25), suggesting

an intercalating mode of binding by pyrene. Also, as illustrated in Figure 25, NH titrations resulted in decreased solution viscosity. At higher ligand concentrations, solution viscosity significantly dropped in both NHP and NH experiments. Such a phenomenon might be explained by an increase in the level of neomycin binding along the DNA grooves, significantly compacting the DNA as mentioned above. The difference in viscometry profiles between the two polymeric DNAs can be a result of stronger pyrene intercalation between the A-T steps in poly(dAdT)₂, stronger neomycin binding to poly(dA)·poly(dT), or a combination of both. Altogether, these studies clearly illustrate neomycin and pyrene's role in the DNA binding event. Multiple spectroscopic experiments have conveyed the Hoechst moiety's presence in DNA binding. Thus, convincing evidence, from a combination of analytical techniques, provides a strong candidacy for a first step in DNA triple recognition agent in NHP.

CONCLUSION

We recently reported that the affinity of neomycin for nucleic acids includes structures known to adopt A-like conformations. We have since endeavored to explore neomycin's utility in binding to B-DNA to improve our understanding of the molecular forces that dictate binding within the DNA major groove. Specifically, a progression from dual recognition to triple recognition has been explored by including an intercalating region (pyrene) within the central spacer separating Hoechst 33258 and neomycin. From the current study of the novel triple recognition agent NHP, the following conclusions can be drawn. (1) NHP significantly enhances DNA stability. UV melting experiments with both polymeric and oligomeric DNA indicate significant shifts in T_m when compared with those of samples in the absence of ligand. The shifts were significantly greater than those with control ligands NP and HPA, indicating contributions by all three binding regions. DSC experiments indicate a significant decrease in the ΔH of duplex melting at the unbound T_m , indicating complexation T_m at a higher temperature (above the limits of instrumental conditions). (2) NHP binds stronger to B-DNA than Hoechst 33258 and other conjugates studied. Fluorescence binding studies with NHP indicate a binding affinity greater than those with Hoechst 33258, NH, and NH with poly(dA)·poly(dT). (3) The mode of binding of Hoechst to DNA is the same in all ligands studied. Circular dichroism experiments indicate similar spectral patterns for poly(dA)·poly(dT) when titrated with either Hoechst 33258 or other Hoechst-neomycin conjugates. (4) The optimal binding site for the conjugates includes a contiguous stretch of nine A-T base pairs. Fluorescence titrations indicated base pair:ligand ratios of 9:1 for NHP. A higher binding constant for NH with poly(dA)·poly(dT) than with Hoechst 33258 was also observed. The importance of the extended A/T site for strong binding was further illustrated in studies with both shorter A/T stretches and interrupted A/T stretches. NHP binding to d(CGCAAATTGCG)₂ exhibited a 10-fold lower binding affinity than Hoechst 33258, yet comparisons with d(CGCAAGCTTGCG)₂ indicate a value for K_b greater than that observed with NH or Hoechst 33258. Such an increase in the level of binding can thus be attributed to intercalation by the pyrene moiety. (5) Pyrene intercalation is apparent using viscometric techniques. Comparison analysis of NHP with NH, Hoechst 33258, and neomycin indicates an increase in solution viscosity when pyrene (in NHP) is present, a phenomenon consistent with DNA intercalation. Altogether,

our results illustrate the first steps in the development of multi-valent (triple recognition) DNA binding molecules. Structural studies and refinement of molecules such as NHP can now be performed to better probe the molecular requirements for multi-recognition of B-DNA.

SUPPORTING INFORMATION AVAILABLE

Synthetic procedures and characterization of all intermediates. This material is available free of charge via the Internet at <http://pubs.acs.org>.

REFERENCES

- Chen, A. Y., Yu, C., Gatto, B., and Liu, L. F. (1993) DNA Minor Groove-Binding Ligands: A Different Class of Mammalian DNA Topoisomerase I Inhibitors. *Proc. Natl. Acad. Sci. U.S.A.* 90, 8131–8135.
- Redinbo, M. R., Champoux, J. J., and Hol, W. G. J. (1999) Structural Insights into the Function of Type IB Topoisomerases. *Curr. Opin. Struct. Biol.* 9, 29–36.
- Redinbo, M. R., Stewart, L., Kuhn, P., Champoux, J. J., and Hol, W. G. J. (1998) *Science* 279, 1504–1513.
- Todd, A. K., Adams, A., Thorpe, J. H., Denny, W. A., Wakelin, L. P. G., and Cardin, C. J. (1999) Major Groove Binding and 'DNA-Induced' Fit in the Intercalation of a Derivative of the Mixed Topoisomerase I/II Poison N-(2-(Dimethylamino)ethyl)acridine-4-carboxamide (DACA) into DNA: X-ray Structure Complexed to d(CG(5-BrU)ACG)₂ at 1.3-Å Resolution. *J. Med. Chem.* 42, 536–540.
- Dervan, P. B. (2001) Molecular Recognition of DNA by Small Molecules. *Bioorg. Med. Chem.* 9, 2215–2235.
- Kielkopf, C. L., Baird, E. E., Dervan, P. B., and Rees, D. C. (1998) Structural Basis for G·C Recognition in the DNA Minor Groove. *Nat. Struct. Biol.* 5, 104–109.
- Kielkopf, C. L., White, S., Szewczyk, J. W., Turner, J. M., Baird, E. E., Dervan, P. B., and Rees, D. C. (1998) A Structural Basis for Recognition of A·T and T·A Base Pairs in the Minor Groove of B-DNA. *Science* 282, 111–115.
- Dickinson, L. A., Trauger, J. W., Baird, E. E., Dervan, P. B., Graves, B. J., and Gottesfeld, J. M. (1999) Inhibition of Ets-1 DNA Binding and Ternary Complex Formation between Ets-1, NF-κB, and DNA by a Designed DNA-Binding Ligand. *J. Biol. Chem.* 274, 12765–12773.
- McBryant, S. J., Baird, E. E., Trauger, J. W., Dervan, P. B., and Gottesfeld, J. M. (1999) Minor Groove DNA-Protein Contacts Upstream of a tRNA Gene Detected with a Synthetic DNA Binding Ligand. *J. Mol. Biol.* 286, 973–981.
- Neely, L., Trauger, J. W., Baird, E. E., Dervan, P. B., and Gottesfeld, J. M. (1997) Importance of Minor Groove Binding Zinc Fingers within the Transcription Factor IIIA-DNA Complex. *J. Mol. Biol.* 274, 439–445.
- Lenzmeier, B. A., Baird, E. E., Dervan, P. B., and Nyborg, J. K. (1999) The Tax Protein-DNA Interaction is Essential for HTLV-I Transactivation in Vitro. *J. Mol. Biol.* 291, 731–744.
- Winston, R. L., Ehley, J. A., Baird, E. E., Dervan, P. B., and Gottesfeld, J. M. (2000) Asymmetric DNA Binding by a Homodimeric bHLH Protein. *Biochemistry* 39, 9092–9098.
- Wurtz, N. R., Pomerantz, J. L., Baltimore, D., and Dervan, P. B. (2002) Inhibition of DNA Binding by NF-κB with Pyrrole-Imidazole Polyamides. *Biochemistry* 41, 7604–7609.
- Weyermann, P., and Dervan, P. B. (2002) Recognition of Ten Base Pairs of DNA by Head-to-Head Hairpin Dimers. *J. Am. Chem. Soc.* 124, 6872–6878.
- Renneberg, D., and Dervan, P. B. (2003) Imidazopyridine/Pyrrole and hydroxybenzimidazole/pyrrole Pairs for DNA Minor Groove Recognition. *J. Am. Chem. Soc.* 125, 5707–5716.
- Bontemps, J., Houssier, C., and Fredericq, E. (1975) Physico-Chemical Study of the Complexes of "33258 Hoechst" with DNA and Nucleohistone. *Nucleic Acids Res.* 2, 971–984.
- Weisblum, B., and Haenssler, E. (1974) Fluorometric Properties of the Bibenzimidazole Derivative Hoechst 33258, a Fluorescent Probe Specific for AT Concentration in Chromosomal DNA. *Chromosoma* 46, 255–260.
- Pilch, D. S., Xu, Z., Sun, Q., Lavoie, E. J., Liu, L. F., Geacintov, N. E., and Breslauer, K. J. (1996) Characterizing the DNA Binding Modes of a Topoisomerase I-Poisoning Terbenzimidazole: Evidence for both

- Intercalative and Minor Groove Binding Properties. *Drug Design Discovery* 13, 115–133.
19. Xu, Z., Li, T. K., Kim, J. S., LaVoie, E. J., Breslauer, K. J., Liu, L. F., and Pilch, D. S. (1998) DNA Minor Groove Binding-Directed Poisoning of Human DNA Topoisomerase I by Terbenzimidazoles. *Biochemistry* 37, 3558–3566.
 20. Aymami, J., Nunn, C. M., and Neidle, S. (1999) DNA Minor Groove Recognition of a Non-Self-Complementary AT-Rich Sequence by a Tris-Benzimidazole Ligand. *Nucleic Acids Res.* 27, 2691–2698.
 21. Wang, L., Bailly, C., Kumar, A., Ding, D., Bajic, M., Boykin, D. W., and Wilson, W. D. (2000) Specific Molecular Recognition of Mixed Nucleic Acid Sequences: An Aromatic Dication that Binds in the DNA Minor Groove as a Dimer. *Proc. Natl. Acad. Sci. U.S.A.* 97, 12–16.
 22. Wang, L., Carrasco, C., Kumar, A., Stephens, C. E., Bailly, C., Boykin, D. W., and Wilson, W. D. (2001) Evaluation of the Influence of Compound Structure on Stacked-Dimer Formation in the DNA Minor Groove. *Biochemistry* 40, 2511–2521.
 23. Wang, L., Kumar, A., Boykin, D. W., Bailly, C., and Wilson, W. D. (2002) Comparative Thermodynamics for Monomer and Dimer Sequence-Dependent Binding of a Heterocyclic Dication in the DNA Minor Groove. *J. Mol. Biol.* 317, 361–374.
 24. Satz, A. L., and Bruice, T. C. (2000) Synthesis of Fluorescent Microgonotropens (FMGTs) and their Interactions with dsDNA. *Bioorg. Med. Chem. Lett.* 8, 1871–1880.
 25. Arya, D. P., and Willis, B. (2003) Reaching into the Major Groove of B-DNA: Synthesis and Nucleic Acid Binding of a Neomycin-Hoechst 33258 Conjugate. *J. Am. Chem. Soc.* 125, 12398–12399.
 26. Willis, B., and Arya, D. P. (2006) Recognition of B-DNA by Neomycin–Hoechst 33258 Conjugates. *Biochemistry* 45, 10217–10232.
 27. Satz, A. L., and Bruice, T. C. (2001) Recognition of Nine Base Pairs in the Minor Groove of DNA by a Tripyrrole Peptide-Hoechst Conjugate. *J. Am. Chem. Soc.* 123, 2469–2477.
 28. Satz, A. L., and Bruice, T. C. (2002) Recognition of Nine Base Pair Sequences in the Minor Groove of DNA at Subpicomolar Concentrations by a Novel Microgonotropen. *Bioorg. Med. Chem.* 10, 241–252.
 29. Satz, A. L., and Bruice, T. C. (1999) Synthesis of a Fluorescent Microgonotropen (FMGT-1) and its Interactions with the Dodecamer d(CCGGAATTCCGG). *Bioorg. Med. Chem. Lett.* 9, 3261–3266.
 30. Sengupta, D., Blasko, A., and Bruice, T. C. (1996) A Microgonotropen Pentaaza Pentabutylamine and its Interactions with DNA. *Bioorg. Med. Chem.* 4, 803–813.
 31. Xi, H., Gray, D., Kumar, S., and Arya, D. P. (2009) Molecular Recognition of Single-Stranded RNA: Neomycin Binding to Poly(A). *FEBS Lett.* 583, 2269–2275.
 32. Willis, B., and Arya, D. P. (2006) Major Groove Recognition of DNA by Carbohydrates. *Curr. Org. Chem.* 10, 663–673.
 33. Willis, B., and Arya, D. P. (2006) An Expanding View of Aminoglycoside-Nucleic Acid Recognition. *Adv. Carbohydr. Chem. Biochem.* 60, 251–302.
 34. Arya, D. P. (2005) Aminoglycoside-Nucleic Acid Interactions: The Case for Neomycin. *Top. Curr. Chem.* 253, 149–178.
 35. Charles, I., and Arya, D. P. (2005) Synthesis of Neomycin-DNA/peptide Nucleic Acid Conjugates. *J. Carbohydr. Chem.* 24, 145–160.
 36. Napoli, S., Carbone, G. M., Catapano, C. V., Shaw, N., and Arya, D. P. (2005) Neomycin Improves Cationic Lipid-Mediated Transfection of DNA in Human Cells. *Bioorg. Med. Chem. Lett.* 15, 3467–3469.
 37. Arya, D. P., Xue, L., and Willis, B. (2003) Aminoglycoside (Neomycin) Preference is for A-Form Nucleic Acids, Not just RNA: Results from a Competition Dialysis Study. *J. Am. Chem. Soc.* 125, 10148–10149.
 38. Arya, D. P., Coffee, R. L., Jr., Willis, B., and Abramovitch, A. I. (2001) Aminoglycoside-Nucleic Acid Interactions: Remarkable Stabilization of DNA and RNA Triple Helices by Neomycin. *J. Am. Chem. Soc.* 123, 5385–5395.
 39. Arya, D. P., Coffee, R. L., Jr., and Charles, I. (2001) Neomycin-Induced Hybrid Triplex Formation. *J. Am. Chem. Soc.* 123, 11093–11094.
 40. Arya, D. P., and Coffee, R. L., Jr. (2000) DNA Triple Helix Stabilization by Aminoglycoside Antibiotics. *Bioorg. Med. Chem. Lett.* 10, 1897–1899.
 41. Arya, D. P., Coffee, R. L., Jr., and Xue, L. (2004) From Triplex to B-Form Duplex Stabilization: Reversal of Target Selectivity by Aminoglycoside Dimers. *Bioorg. Med. Chem. Lett.* 14, 4643–4646.
 42. Arya, D. P. (2007) Aminoglycoside Antibiotics: From Chemical Biology to Drug Discovery, Wiley-Interscience, Hoboken, NJ.
 43. Xue, L., Charles, I., and Arya, D. P. (2002) Neomycin-Pyrene Conjugate: Dual Modes of Triplex Recognition. *Chem. Commun.*, 70–71.
 44. Arya, D. P., Xue, L., and Tennant, P. (2003) Combining the Best in Triplex Recognition: Synthesis and Nucleic Acid Binding of a BQQ-Neomycin Conjugate. *J. Am. Chem. Soc.* 125, 8070–8071.
 45. Shaw, N. N., Xi, H., and Arya, D. P. (2008) Molecular Recognition of a DNA:RNA Hybrid: Sub-Nanomolar Binding by a Neomycin-Methidium Conjugate. *Bioorg. Med. Chem. Lett.* 18, 4142–4145.
 46. Shaw, N. N., and Arya, D. P. (2008) Recognition of the Unique Structure of DNA:RNA Hybrids. *Biochimie* 90, 1026–1039.
 47. Charles, I., Xue, L., and Arya, D. P. (2002) Synthesis of Aminoglycoside-DNA Conjugates. *Bioorg. Med. Chem. Lett.* 12, 1259–1262.
 48. Charles, I., Xi, H., and Arya, D. P. (2007) Sequence-Specific Targeting of RNA with an Oligonucleotide-Neomycin Conjugate. *Bioconjugate Chem.* 18, 160–169.
 49. Willis, B., and Arya, D. P. (2009) Triple Recognition of B-DNA. *Bioorg. Med. Chem. Lett.* 19, 4974–4979.
 50. Bordonel, J. A., Feierabend, K. J., Siddiqui, S. A., Wright, L. L., and Petty, J. T. (2002) Viscometry and Atomic Force Microscopy Studies of the Interactions of a Dimeric Cyanine Dye with DNA. *J. Phys. Chem. B* 106, 4838–4843.
 51. Spink, N., Brown, D. G., Skelly, J. V., and Neidle, S. (1994) Sequence-Dependent Effects in Drug-DNA Interaction: The Crystal Structure of Hoechst 33258 Bound to the d(CGAAATTCGCG)2 Duplex. *Nucleic Acids Res.* 22, 1607–1612.
 52. Kaul, M., Barbieri, C. M., Kerrigan, J. E., and Pilch, D. S. (2003) Coupling of Drug Protonation to the Specific Binding of Aminoglycosides to the A Site of 16 S rRNA: Elucidation of the Number of Drug Amino Groups Involved and their Identities. *J. Mol. Biol.* 326, 1373–1387.
 53. Botto, R. E., and Coxon, B. (1983) Nitrogen-15 Nuclear Magnetic Resonance Spectroscopy of Neomycin B and Related Aminoglycosides. *J. Am. Chem. Soc.* 105, 1021–1028.
 54. Geacintov, N. E., Shahbaz, M., Ibanez, V., Moussaoui, K., and Harvey, R. G. (1988) Base-Sequence Dependence of Noncovalent Complex Formation and Reactivity of Benzo[a]Pyrene Diol Epoxide with Polynucleotides. *Biochemistry* 27, 8380–8387.
 55. Pjura, P. E., Grzeskowiak, K., and Dickerson, R. E. (1987) Binding of Hoechst 33258 to the Minor Groove of B-DNA. *J. Mol. Biol.* 197, 257–271.
 56. Loontiens, F. G., Regenfuss, P., Zechel, A., Dumortier, L., and Clegg, R. M. (1990) Binding Characteristics of Hoechst 33258 with Calf Thymus DNA, Poly[d(A-T)], and d(CCGGAATTCCGG): Multiple Stoichiometries and Determination of Tight Binding with a Wide Spectrum of Site Affinities. *Biochemistry* 29, 9029–9039.
 57. Breusegem, S. Y., Clegg, R. M., and Loontiens, F. G. (2002) Base-Sequence Specificity of Hoechst 33258 and DAPI Binding to Five (A/T)₄ DNA Sites with Kinetic Evidence for More than One High-Affinity Hoechst 33258-AATT Complex. *J. Mol. Biol.* 315, 1049–1061.
 58. Breusegem, S. Y., Loontiens, F. G., Regenfuss, P., and Clegg, R. M. (2001) Kinetics of Binding of Hoechst Dyes to DNA Studied by Stopped-Flow Fluorescence Techniques. *Methods Enzymol.* 340, 212–233.
 59. Loontiens, F. G., McLaughlin, L. W., Diekmann, S., and Clegg, R. M. (1991) Binding of Hoechst 33258 and 4',6'-Diamidino-2-phenylindole to Self-Complementary Decadeoxynucleotides with Modified Exocyclic Base Substituents. *Biochemistry* 30, 182–189.
 60. Macgregor, R. B., Jr., Clegg, R. M., and Jovin, T. M. (1985) Pressure-Jump Study of the Kinetics of Ethidium Bromide Binding to DNA. *Biochemistry* 24, 5503–5510.
 61. Bostock-Smith, C. E., and Searle, M. S. (1999) DNA Minor Groove Recognition by Bis-Benzimidazole Analogs of Hoechst 33258: Insights into Structure-DNA Affinity Relationships Assessed by Fluorescence Titration Measurements. *Nucleic Acids Res.* 27, 1619–1624.
 62. Haq, I. (2002) Thermodynamics of Drug-DNA Interactions. *Arch. Biochem. Biophys.* 403, 1–15.
 63. Arya, D. P., Coffee, R. L., and Xue, L. (2004) From Triplex to B-Form Duplex Stabilization: Reversal of Target Selectivity by Aminoglycoside Dimers. *Bioorg. Med. Chem. Lett.* 14, 4643–4646.
 64. Rao, K. E., and Lown, J. W. (1991) Molecular Recognition between Ligands and Nucleic Acids: DNA Binding Characteristics of Analogs of Hoechst 33258 Designed to Exhibit Altered Base and Sequence Recognition. *Chem. Res. Toxicol.* 4, 661–669.
 65. Canzonetta, C., Caneva, R., Savino, M., Scipioni, A., Catalanotti, B., and Galeone, A. (2002) Circular Dichroism and Thermal Melting Differentiation of Hoechst 33258 Binding to the Curved (A₄T₄) and Straight (T₄A₄) DNA Sequences. *Biochim. Biophys. Acta* 1576, 136–142.
 66. Chen, F. M. (1983) Binding of Pyrene to DNA, Base Sequence Specificity and its Implication. *Nucleic Acids Res.* 11, 7231–7250.

67. Hartley, J. A., Webber, J., Wyatt, M. D., Bordenick, N., and Lee, M. (1995) Novel Cytotoxic DNA Sequence and Minor Groove Targeted Photosensitizers: Conjugates of Pyrene and Netropsin Analogues. *Bioorg. Med. Chem.* 3, 623–629.
68. Cohen, G., and Eisenberg, H. (1969) Viscosity and Sedimentation Study of Sonicated DNA-Proflavine Complexes. *Biopolymers* 8, 45–55.
69. Arya, D. P., Micovic, L., Charles, I., Coffee, R. L., Jr., Willis, B., and Xue, L. (2003) Neomycin Binding to Watson-Hoogsteen (W-H) DNA Triplex Groove: A Model. *J. Am. Chem. Soc.* 125, 3733–3744.
70. Jin, E., Katritch, V., Olson, W. K., Kharatishvili, M., Abagyan, R., and Pilch, D. S. (2000) Aminoglycoside Binding in the Major Groove of Duplex RNA: The Thermodynamic and Electrostatic Forces that Govern Recognition. *J. Mol. Biol.* 298, 95–110.